Computational motor control: feedback and accuracy

Emmanuel Guigon, Pierre Baraduc, Michel Desmurget

Computational motor control: Feedback and accuracy

Emmanuel Guigon [1], Pierre Baraduc [2], Michel Desmurget [2]
[1] INSERM U742, ANIM
Université Pierre et Marie Curie (UPMC – Paris 6)
9, quai Saint-Bernard, 75005 Paris, France
[2] Centre de Neurosciences Cognitives, CNRS UMR 5229,
67, Bd Pinel, 69675 Bron, France

Running title: Optimal motor control

Correspondence to:
Emmanuel Guigon
INSERM U742, ANIM
U.P.M.C., Boîte 23
9, quai Saint-Bernard
75005 Paris, France
Fax: 33 1 44 27 34 38
Tel: 33 1 44 27 34 37
Email: guigon@ccr.jussieu.fr

47 pages / 9 figures / 0 table / 33 equations
Number of words: whole = 12348 / abstract = 187 / introduction = 327

Keywords: Modeling; Motor; Noise

European Journal of Neuroscience, in press (december 2007)

Abstract

Speed/accuracy trade-off is a ubiquitous phenomenon in motor behavior, which has been ascribed to the presence of signal-dependent noise in motor commands. Although this explanation can provide a quantitative account of many aspects of motor variability, including Fitts' law, the fact that this law is frequently violated, e.g. during the acquisition of new motor skills, remains unexplained. Here, we describe a principled approach to the influence of noise on motor behavior, in which motor variability results from the interplay between sensory and motor execution noises in an optimal feedback-controlled system. In this framework, we first show that Fitts' law arises due to signal-dependent motor noise when sensory (proprioceptive) noise is low, e.g. under visual feedback. Then we show that the terminal variability of nonvisually guided movement can be explained by the presence of signal-dependent proprioceptive noise. Finally, we show that movement accuracy can be controlled by opposite changes in signal-dependent sensory and motor noise, a phenomenon which could be ascribed to muscular cocontraction. As the model also explains kinematics, kinetics, muscular, and neural characteristics of reaching movements, it provides a unified framework to address motor variability.

Variability in performance is an ubiquitous phenomenon in motor behaviors (Woodworth, 1899; Fitts, 1954). It reflects the corruption of movement planning and execution processes by noise in sensory feedback and motor commands (Schmidt *et al.*, 1979; Meyer *et al.*, 1988; Hoff & Arbib, 1993; Harris & Wolpert, 1998; Todorov & Jordan, 2002; van Beers *et al.*, 2002, 2004; Todorov, 2005). Both types of noise influence the accuracy of motor acts, but in a seemingly different way. On the one hand, uncertainty in sensory signals directly translates into performance variability (van Beers *et al.*, 2002). Noise in sensory inputs is the main determinant of precision in smooth pursuit eye movements (Osborne *et al.*, 2005). Furthermore, statistics of sensory noise are taken into account in motor planning (Baddeley *et al.*, 2003). On the other hand, the effect of noisy motor commands is more versatile. The presence of signal-dependent motor noise (i.e. noise whose variance increases with the size of the commands) results in a speed/accuracy trade-off: faster movements require larger commands, and thus endure more noise and more variability (Meyer *et al.*, 1988; Harris & Wolpert, 1998). Yet, increased muscular cocontraction during movement results in more variable command signals (electromyograms, joint torques; Osu *et al.*, 2004) as expected from the presence of signal-dependent noise, but also improved movement accuracy (Laursen *et al.*, 1998; Seidler-Dobrin *et al.*, 1998; Gribble *et al.*, 2003; Osu *et al.*, 2004; Visser *et al.*, 2004; Sandfeld & Jensen, 2005; van Roon *et al.*, 2005).

This “speed/accuracy” paradox is a central, but unexplained issue. The role of cocontraction and the fact that improved accuracy can be observed in the absence of visual feedback (Seidler-Dobrin *et al.*, 1998; Osu *et al.*, 2004) suggest that proprioceptive feedback could play a role in the control of movement accuracy. In this article, we show in a model that the influence of noise in proprioceptive feedback could be a key factor to explain the “speed/accuracy” paradox in human motor behavior.

Materials and Methods

General principle

We considered the dynamical systems approach to the description of motor control (Wolpert & Ghahramani, 2000; Todorov & Jordan, 2002; Saunders & Knill, 2004; Guigon *et al.*, 2007, 2008). In this framework, motor control is viewed as the mastering of a state-dependent dynamics in the presence of state- and control-dependent noise (Todorov, 2005). We used the structure of noise-induced variability to probe the nature and influence of noise on motor control.

To illustrate, we consider a simple example: an inertial point which can move along a line, actuated by a force generator (Fig. 1*A*). The force generator transmits a control input $u(t)$ (in fact a force), which is translated into a displacement $x(t)$. The goal is to find the control which displaces the mass from position x_0 at time t_0 to position x_f at time t_f, with two constraints: 1. the control is noisy (presence of *motor noise*); 2. the state of the inertial point (position $x(t)$, velocity) is not known, but can only be observed ($y(t)$) through a noisy sensor (presence of *sensory noise*), and estimated (estimation is denoted $\hat{x}(t)$). At each time t, the control is calculated as a function of the estimated distance to the goal $x_f - \hat{x}(t)$. Over repeated trials, the resulting trajectory will be each time different (Fig. 1*B*), reflecting the structure and strength of sensory and motor noises. The set of trajectories $x^i(t)$ ($t \in [t_0;t_f]$, $i = 1 \ldots N$; N number of trials) can be analyzed to reveal the structure of variability (e.g. time course of variance, final variability, …) in order to compare with experimental data (Gordon *et al.*, 1994a; van Beers *et al.*, 2004). This example contains basic components for the study of motor variability.

A classical solution to this problem can be obtained using a stochastic optimal feedback controller (Todorov & Jordan, 2002), i.e. a controller which simultaneously minimizes the size

of the control (*effort*) and the distance to the goal (*error*), taking into account the statistics of sensory and motor noise, coupled with an optimal state estimator (a Kalman filter, which provides an optimal state estimate based on efference copy of motor commands and sensory feedback). The rationale for this choice has been thoroughly elaborated in recent publications (Todorov & Jordan, 2002; Scott, 2004; Todorov, 2004). Briefly, optimality provides an efficient solution to kinematic and muscular redundancy, and stochastic feedback control guarantees flexible and versatile compensations for internal and external perturbations (noise, target displacement, …; Todorov & Jordan, 2002). A drawback of this approach arises from the minimization of a mixed error/effort cost function. Such a minimization requires the setting of parameters which weight the contribution of state errors (position, velocity, force, ...) and effort in the cost function. Since different settings lead to different behaviors, such a model cannot provide a univocal description of motor control. To circumvent this difficulty, we used a slightly different model which treats error and effort separately (Guigon *et al.*, 2007a, 2008). We have shown previously that this model can properly address redundancy (Guigon *et al.*, 2007a), and motor variability (Guigon *et al.*, 2008).

Central idea

The goal of our work is to address speed/accuracy trade-off in motor behavior. But it has not yet been shown that optimal feedback control can address Fitts' law. Previous studies have shown that Fitts' law can arise from a minimum variance model (Harris & Wolpert, 1998; Tanaka *et al.*, 2006), i.e. an open-loop model which constrains the size of terminal variance in the presence of motor noise (signal-dependent motor noise, SDN_m). There are two ways to consider the relationship between minimum variance and optimal feedback control models. On the one hand, as the former model is open-loop, we could consider an "open-loop" version of optimal feedback control, i.e. when the optimal state estimator does not receive sensory

feedback (where sensory feedback is defined as visual and proprioceptive feedback from the moving apparatus). Yet such a model can hardly be considered as a model of normal motor control (it could be considered as a model of deafferentation). On the other hand, the minimum variance model could be considered as an optimal way to compensate for SDN_m in the absence of other perturbations. As sensory noise decreases toward zero, optimal feedback control could also be considered as an optimal way to compensate for SDN_m in the absence of other perturbations. Yet the zero-noise case (i.e. perfect sensory feedback) should lead to instantaneous compensation of motor noise and zero variability (the gain of the Kalman filter becomes infinite). This case is not realistic as sensory delays preclude instantaneous corrections. To approach the condition of "perfect sensory feedback", we used a small signal-independent sensory noise (see definition below) which precluded instantaneous corrections (the Kalman gain remains bounded), but produced little variability. In the following, we used the term "perfect sensory feedback" to refer to this condition. In this framework, the equivalence between minimum variance and optimal feedback control could be related to the fact the two models attempt to find the smallest motor commands in order to reduce the quantity of SDN_m.

Hypotheses and simplifications

Origin of variability

A central issue in the study of motor variability is the origin of this variability. Several studies have ascribed variability to the movement planning process (Gordon *et al.*, 1994a; McIntyre *et al.*, 1997; Vindras & Viviani, 1998). However, no authoritative demonstration has been provided to support this idea. Furthermore, computational studies have shown that characteristic features of motor variability (e.g. shape of terminal variability ellipses, time

course of variability along a trajectory, …) can be quantitatively explained by a noisy execution process (Todorov & Jordan, 2002; van Beers *et al.*, 2004). In fact, it seems that, in many conditions, planning-related variability is much smaller than execution-related variability (discussion in van Beers *et al.*, 2004; but see Churchland *et al.*, 2006). Here, we retained this idea, and focused on the influence of execution noise.

Nature of noise

Since neither the origin nor the nature of noise can be precisely determined, a principled approach to the structure of noise was used (Saunders & Knill, 2004; Todorov, 2005): 1. Noise corrupts both motor commands and sensory feedback signals; 2. Noise has additive (signal-independent, SIN), and multiplicative (signal-dependent, SDN) effects. SDN is described by its variance

$$\sigma^2 = k \mid u \mid^p,$$

where u is the signal, and k and p are constants. An open question is the value of the exponent p. In modeling studies (Harris & Wolpert, 1998; Todorov & Jordan, 2002; Tanaka *et al.*, 2004, 2006), it is in general assumed that $p = 2$ in agreement with some experimental observations (Jones *et al.*, 2002; Todorov, 2002). Yet, other studies have reported a lower p (Laidlaw *et al.*, 2000; Christou & Carlton, 2002; see discussion in Stein *et al.*, 2005). Interestingly, Iguchi *et al.* (2005) have shown that predictions of the minimum variance model (Harris & Wolpert, 1998) depend on p. In particular, Fitts' law was found only for $p = 2$. Here, we used $p = 2$, but we explored consequences of this choice for the reported results.

Nature of feedback

Control of limb movements involves both visual and proprioceptive feedback. Movement

accuracy depends on noise characteristics and time delays in each feedback modality. Here, we were interested in the role of proprioceptive feedback. Thus, we built a model of noisy proprioception to explore variability of movements of the unseen limb (e.g. Gordon *et al.*, 1994a; van Beers *et al.*, 2004). To compare visually-guided and nonvisually-guided movements (in the study of Fitts' law), we assumed that visual feedback can be represented by a perfect sensory feedback (as defined above). The rationale for this hypothesis is related to the equivalence (for the study of Fitts' law) between optimal feedback control and a minimum variance model in the presence of perfect sensory feedback (see above).

In this way, we considered a single source of feedback, and we varied the strength of noise to simulate different configurations: 1. Zero signal-dependent sensory noise for movement with visual feedback. This simplification is based on the fact that the state estimator weights feedback modalities according to their precision. Thus the state estimator would nearly ignore proprioceptive feedback in the presence of vision; 2. Nonzero signal-dependent sensory noise for movement without visual feedback. Below, we use either the generic term "sensory feedback", or proprioceptive (resp. visual) feedback to indicate noisy (resp. perfect) sensory feedback.

Nature of the model

In this article, we considered two control problems: 1. an inertial point in two-dimensional space actuated by two linear muscles (*linear* model). This model has proven adequate to address motor variability in various conditions (Todorov & Jordan, 2002). Furthermore, it can be solved analytically (Guigon *et al.*, 2008), and is thus appropriate for in-depth evaluations, e.g. to study the influence of parameters; 2. a planar articulated arm actuated by two pairs of nonlinear antagonist muscles (*nonlinear* model). When the spatial structure of variability is addressed, the use of the linear model is not easy to justify, and the more realistic, nonlinear model was

used to confirm the results obtained with the linear model.

Notations

In the following, dx/dt and d^2x/dt^2 denote the first and second derivative of $x(t)$ relative to t. Vectors are indicated by bold letters (**x**), and matrices by uppercase underlined letters ($\underline{A}$). Diag() denotes a diagonal matrix built from the numbers between the parentheses. We define $\underline{I}_n$ as the n-dimensional identity matrix. We also define $\underline{J}_2$ as

0	1
-1	0

and L_1, L_2, L_3, L_4 as

1	1	1	-1
1	1	1	-1
1	1	1	-1
1	1	1	-1

1	1	-1	1
1	1	-1	1
1	1	-1	1
1	1	-1	1

1	-1	1	1
1	-1	1	1
1	-1	1	1
1	-1	1	1

-1	1	1	1
-1	1	1	1
-1	1	1	1
-1	1	1	1

Mathematical formulation: optimal feedback control

The dynamics of the moving apparatus was described by a continuous noisy system

$$d\mathbf{x}/dt = f(\mathbf{x}(t),\mathbf{u}(t)) + \mathbf{noise}_{dyn}(t), \quad \text{(Eq. 1)}$$

where $\mathbf{x}$ is a n-dimensional *state* vector, $\mathbf{u}$ a m-dimensional *control* vector, $\mathbf{noise}_{dyn}$ a n-dimensional noise on the dynamics (see below). State was not directly observable, but was obtained through noisy observation

$$\mathbf{y}(t) = \underline{H}\mathbf{x}(t) + \mathbf{noise}_{obs}(t), \quad \text{(Eq. 2)}$$

where $\mathbf{y}$ is a p-dimensional *observation* vector (sensory feedback), $\underline{H}$ a p×n observation matrix, and $\mathbf{noise}_{obs}$ a p-dimensional noise on the observation (see below). A state estimate $\hat{\mathbf{x}}$ was built through optimal estimation (Kalman filtering)

$$d\hat{\mathbf{x}}/dt = f(\hat{\mathbf{x}}(t),\mathbf{u}(t)) + \underline{K}(t)\,[\mathbf{y}(t) - \underline{H}\hat{\mathbf{x}}(t)], \quad \text{(Eq. 3)}$$

where $\underline{K}$ is the n×p Kalman gain matrix (Guigon *et al.*, 2008). The meaning of Eq. 3 is the following. The next estimated state can be obtained from: 1. an internal simulation of the dynamics, i.e. a forward model (first term in the right-hand side of Eq. 3); 2. sensory inputs (second term term in the right-hand side of Eq. 3). For optimal estimation, the two terms are combined according the maximum likelihood principle, i.e. each term has a weight which is inversely proportional to its variance. The weighting is represented here by $\underline{K}$.

Delayed feedback (Δ) was introduced in the *linear* model (see below) as described by Todorov & Jordan (2002) (their Supplementary Information). Since simulations with reasonable delays (e.g., $\Delta = 100$ ms) were highly time consuming [~3 h to calculate variability statistics ($N = 500$ trials) of a single movement; ~1,600 movements were simulated to build Fig. 2], full results were first obtained without delay, and then confirmed with nonzero delay in

a subset of cases.

Both dynamics and observation were corrupted by noise (Todorov, 2005). We had

$$\mathbf{noise}_{dyn}(t) = \xi(t) + \sum_{i=1..c} \varepsilon_i(t)\, \underline{C}_i\, \mathbf{u}(t), \qquad \text{(Eq. 4)}$$

where ξ is a n-dimensional zero-mean Gaussian random vector with covariance matrix Ω^{ξ}, $\varepsilon = [\varepsilon_1 \ldots \varepsilon_c]$ a zero-mean Gaussian random vector with covariance matrix Ω^{ε}, and $[\underline{C}_1 \ldots \underline{C}_c]$ a set of n×m matrices. The former type of noise is called SIN_m (signal-independent motor noise). The latter is known as SDN_m (signal-dependent motor noise). In the same way,

$$\mathbf{noise}_{obs}(t) = \omega(t) + \sum_{l=1..d} \zeta_i(t)\, \underline{D}_i\, \mathbf{x}(t), \qquad \text{(Eq. 5)}$$

where ω is a p-dimensional zero-mean Gaussian random vector with covariance matrix Ω^{ω}, $\zeta = [\zeta_1 \ldots \zeta_d]$ a zero-mean Gaussian random vector with covariance matrix Ω^{ζ}, and $[\underline{D}_1 \ldots \underline{D}_d]$ a set of m×n matrices. The former type of noise is called SIN_s (signal-independent sensory noise). The latter is termed SDN_s (signal-dependent sensory noise).

An optimal feedback control problem for the system defined by Eqs. 1-5 is to find a control vector **u** at time $t \in [t_0;t_f]$ to minimize a performance index (E, effort)

$$E^2 = \sum_{i=1..m} \int_{[t\,;\,t_f]} u_i^2(w)\, dw$$

subject to Eq. 1, with boundary conditions $\mathbf{x}_t$ and $\mathbf{x}_f$. Initial boundary condition is $\mathbf{x}_t = \hat{\mathbf{x}}(t)$, i.e. estimated state at time t, for movement planning, and $\mathbf{x}_t = \mathbf{x}(t)$, i.e. actual state at t, for execution. A complete movement is obtained as a solution to this problem for each time t in $[t_0;t_f]$ (discretization step δ).

The functioning of the model is summarized in Fig. 2. The model contains a controller (an

optimal feedback controller as explained above), a state estimator (Eqs. 2,3), and a controlled object (the moving apparatus). At each time step, the controller elaborates a control signal based on the target state and the estimated state of the controlled object. The control signal is transmitted to the controlled object which evolves according to its dynamics (Eq. 1). State estimation results from a weighted combination of a control-based estimation (forward model) and a sensory-based correction (Kalman filter).

Linear case

The moving apparatus was an inertial point in two-dimensional space actuated by two muscles (n = 8, m = 2). The dynamics was

$$\underline{M}\, d^2\mathbf{q}/dt^2 = \mathbf{F},$$

where $\mathbf{q} = [q_1\ q_2]^T$ is the position of the point, $\underline{M} = [m_1\ 0;\ 0\ m_2]$ the inertia matrix, and $\mathbf{F} = [F_1\ F_2]^T$ contains the forces exerted by the muscles. Each muscle i was modeled as a second-order linear filter which transforms a neural control signal (u_i) into a muscular force (F_i) according to

$$\nu\, de_i/dt = -e_i + u_i \text{ (excitation)}$$

$$\nu\, da_i/dt = -a_i + e_i \text{ (activation)} \qquad \text{(Eq. 6)}$$

$$F_i = \eta(a_i)$$

where ν is a time constant, and $\eta(z) = z$. The state vector was

$$\mathbf{x} = [q_1(t);q_2(t);dq_1(t)/dt;dq_2(t)/dt;a_1(t);a_2(t);e_1(t);e_2(t)].$$

Thus

$$f(\mathbf{x}(t),\mathbf{u}(t)) = \underline{A}\mathbf{x}(t) + \underline{B}\mathbf{u}(t),$$

where the matrix $\underline{A}$ was

0	0	1	0	0	0	0	0
0	0	0	1	0	0	0	0
0	0	0	0	$1/m_1$	0	0	0
0	0	0	0	0	$1/m_2$	0	0
0	0	0	0	$-1/\nu$	0	$1/\nu$	0
0	0	0	0	0	$-1/\nu$	0	$1/\nu$
0	0	0	0	0	0	$-1/\nu$	0
0	0	0	0	0	0	0	$-1/\nu$

and $\underline{B}$ was

0	0
0	0
0	0
0	0
0	0
0	0
$1/\nu$	0
0	$1/\nu$

The optimal feedback control problem was solved analytically as explained in Guigon *et al.* (2008), and simulated numerically.

General parameters

We used $\nu = 40$ ms, $\delta = 1$ ms. To represent the inertial anisotropy of a real arm (Hogan, 1985), we used $m_1 = 2$ kg and $m_2 = 1$ kg.

Motor noise

Signal-dependent motor noise (Eq. 4). We chose $c = 2$,

$$\underline{C}_1 = \underline{B}\,\underline{I}_2 \qquad \underline{C}_2 = \underline{B}\,\underline{J}_2,$$

and

$$\Omega^{\varepsilon} = \sigma_{SDNm}\, \underline{I}_2,$$

where σ_{SDNm} is the s.d. of noise (see Todorov & Jordan, 2002). The rationale for this choice (circular covariance) is to obtain independent noise of similar variance on the two dimensions.

Signal-independent motor noise (Eq. 4). To assess the specific role of SDN_m, signal-independent motor noise (SIN_m) was used with

$$\Omega^{\xi} = \sigma_{SINm}\, \mathrm{Diag}(0,0,0,0,0,0,1,1),$$

where σ_{SINm} is the s.d. of noise.

Simulation of nonvisually guided movements

Observation matrix (Eq. 2). The structure of the observation process should reflect the nature of biological sensors which provide measures of state-related quantities. In physiological terms, the observation matrix corresponds to the integrated contribution of proprioceptive and cutaneous receptors (muscle spindles, Golgi tendon organs, articular receptors, …; Burgess *et al.*, 1982) to kinesthetic movement detection. However, this process is distributed, complex, nonlinear, and cannot be exactly represented in a linear framework. Here, the main simplifying assumption is that state can be directly and exactly measured from the sensors (in the absence of noise). Although this assumption is not easy to justify on physiological ground, it is well demonstrated that human subjects can measure and manipulate states (e.g. positions, velocities, forces; Ghahramani *et al.*, 1996; Kerr & Worringham, 2002; Todorov, 2002). The simplest structure for $\underline{H}$ is

$$\mathrm{Diag}(1,1,1,1,1,1,1,1),$$

corresponding to $p = n = 8$, i.e. the full state is observable. To assess the influence of the structure of the observation matrix on the results, we considered cases where some parts of the

state vector were not observable (see **Results**). In particular, it is unclear whether excitation (roughly the derivative of force) is measured by sensors. Since the model is a highly simplified, linear representation of complex processes (e.g. Hasan, 1983), our goal is not to draw firm conclusions on the nature of feedback information, but to address conditions in which our results remain valid.

Signal-dependent sensory noise (Eq. 5). There are many possible configurations for SDN_s, and all configurations cannot be systematically tested. In fact, there are two extreme configurations. The first corresponds to the less favorable case for a structured variability to emerge, i.e. each state is a source of noise, and all the sources of noise are independent. In this case, d = 8, and

$$\underline{D}_1 = \mathrm{Diag}(1,0,0,0,0,0,0,0) \ldots \underline{D}_8 = \mathrm{Diag}(0,0,0,0,0,0,0,1).$$

In the second configuration, there is a single source of noise for all states. In this case, d = 1, and

$$\underline{D}_1 = \mathrm{Diag}(1,1,1,1,1,1,1,1).$$

The true configuration (in the framework of our simplified model) is somewhere between these extremes. As an intermediate configuration, we considered the case where there is a single source of noise for each type of state (position, velocity, activation, excitation), i.e. d = 4, and

$$\underline{D}_1 = \mathrm{Diag}(1,1,0,0,0,0,0,0) \ldots \underline{D}_4 = \mathrm{Diag}(0,0,0,0,0,0,1,1).$$

In the three cases,

$$\Omega^{\zeta} = \sigma_{SDNs}\, \underline{I}_d,$$

where σ_{SDNs} is the s.d. of noise. The intermediate configuration was used as the default configuration, and the two extreme configurations were used to assess the influence of the

structure of noise on the results. The highly simplified nature of the model does not authorize a more thorough analysis of the structure of noise.

Signal-independent sensory noise (Eq. 5). To assess the specific role of SDN_s, signal-independent sensory noise (SIN_s) was used with

$$\Omega^{\omega} = \sigma_{SINs}\ \mathrm{Diag}(0.1,0.1,1,1,10,10,100,100),$$

where σ_{SINs} is the s.d. of noise.

Simulation of visually guided movements

We set σ_{SDNs} to 0.

Nonlinear case

The moving apparatus was a two-joint planar arm (shoulder/elbow) actuated by two pairs of antagonist muscles (n = 12, m = 4). The dynamics was

$$\underline{\mathrm{In}}(\mathbf{q})\ d^2\mathbf{q}/dt^2 + \underline{\mathrm{Cor}}\ (\mathbf{q},d\mathbf{q}/dt) = \mathbf{T}, \qquad \text{(Eq. 7)}$$

where $\mathbf{q} = [q_1\ q_2]^T$ are the joint angles, $\underline{\mathrm{In}}$ the position-dependent inertia matrix, $\underline{\mathrm{Cor}}$ the matrix of Coriolis and centripetal forces, and **T** the torques generated by muscle forces (Guigon *et al.*, 2007a). The muscles were modeled as described by Eq. 6 with $\eta(z) = [z]^+$. The state vector was

$$\mathbf{x}(t) = [q_1(t),q_2(t),dq_1(t)/dt,dq_2(t)/dt,a_1(t),a_2(t),a_3(t),a_4(t),e_1(t),e_2(t),e_3(t),e_4(t)],$$

and function $f(\mathbf{x}(t),\mathbf{u}(t))$ was obtained from Eq. 6 and Eq. 7. The optimal feedback control was derived analytically as explained in Guigon *et al.* (2008), and then simulated numerically as explained in Guigon *et al.* (2007a).

This model is a simplified model which does not take into account the complex nonlinear behavior of muscles and the presence of biarticular muscles (see Guigon *et al.*, 2007b for a

more general model). Yet, it was deemed sufficient for the present purpose (see Guigon *et al.*, 2007a for a discussion).

General parameters

They can be found in Guigon *et al.* (2007a).

Motor noise

Signal-dependent motor noise (Eq. 4). We chose c = 4,

$$\underline{C}_1 = \underline{B}\,\underline{L}_1 \qquad \underline{C}_2 = \underline{B}\,\underline{L}_2 \qquad \underline{C}_3 = \underline{B}\,\underline{L}_3 \qquad \underline{C}_4 = \underline{B}\,\underline{L}_4,$$

where $\underline{B} = \partial f/\partial \mathbf{u}$, to obtain independent noise of similar variance on the four dimensions.

Signal-independent motor noise (Eq. 4). We used

$$\Omega^{\xi} = \sigma_{SINm}\,\mathrm{Diag}(0,0,0,0,0,0,0,0,1,1,1,1).$$

Simulation of nonvisually-guided movements

Observation matrix (Eq. 2). The nonlinear model was only used to simulate nonvisually-guided movements. The observation matrix was

$$\mathrm{Diag}(1,1,1,1,1,1,1,1,1,1,1,1),$$

corresponding to p = n = 12.

Signal-dependent sensory noise (Eq. 5). We used d = 4, and

$$\underline{D}_1 = \mathrm{Diag}(1,1,0,0,0,0,0,0,0,0,0,0) \qquad \underline{D}_2 = \mathrm{Diag}(0,0,1,1,0,0,0,0,0,0,0,0)$$

$$\underline{D}_3 = \mathrm{Diag}(0,0,0,0,1,1,1,1,0,0,0,0) \qquad \underline{D}_4 = \mathrm{Diag}(0,0,0,0,0,0,0,0,1,1,1,1).$$

Signal-independent sensory noise (Eq. 5). We used

$$\Omega^{\omega} = \sigma_{SINs}\ \mathrm{Diag}(0.01,0.01,0.1,0.1,1,1,1,1,10,10,10,10).$$

Quantitative description of variability

Behavioral variability is in general described by a systematic error (bias), and a random error. Ideally, these errors should be referred to as accuracy and precision, respectively (Bevington, 1969). Yet these terms have been used interchangeably in the literature (e.g. speed/accuracy trade-off). Here, we are interested only with random errors, and we will use the terms variability and accuracy for their description.

Terminal variability was described by characteristics of the 95% equal frequency ellipse (i.e. the ellipse which contains, on average, 95% of endpoints, calculated over *N* trials; Sokal & Rohlf, 1995; see Fig. 3*B*, inset): 1. its surface area (in cm^2), and the square root of its surface area (Ω, in cm); 2. its orientation (θ, in deg): the angle of the major axis of the ellipse relative to movement direction; 3. its aspect ratio (ellipse elongation): the ratio λ_1/λ_2, where the quantities λ_1 and λ_2 ($\lambda_1 \geq \lambda_2$) are the square root of the eigenvalues of the covariance matrix of endpoint distribution.

Results

Unless otherwise mentioned, the results were obtained using the linear model with $p = 2$ (exponent of signal-dependent noise).

General properties of the model

We first note that the model reproduces basic expected characteristics of motor behavior. Simulated trajectories were straight with a bell-shaped velocity profile (Fig. 3*A*,*B*). A typical control signal had an early phasic component followed by a depression (Fig. 3*C*), and resembled the discharge pattern of EMG-like neurons found in primate motor cortex (Sergio & Kalaska,

1998; see Guigon *et al.*, 2007b). A typical excitation signal had a triphasic agonist/antagonist pattern (Fig. 3*D*; the agonist and antagonist bursts are found on the same trace since there is a single control per Cartesian direction), similar to EMG patterns of fast reaching movements. In fact, we have shown elsewhere that the model can accurately account for kinematics, kinetics, muscular, and neural characteristics of reaching movements (Guigon *et al.*, 2007a,b).

What is the origin of Fitts' law?

The starting point of our reasoning is Fitts' law. This law writes

$$MT = a + b \log_2(2A/W), \qquad \text{(Eq. 8)}$$

where MT is movement duration (in ms), A movement amplitude (in cm), and W target width (in cm). This relationship contains two parts: a scaling law (between amplitude and duration) and a speed/accuracy trade-off (between duration and target width). Although each part is easy to explain on its own, models show that the coordination in a single rule is probably a complex, emergent property of neural motor control (Meyer *et al.*, 1988; Harris & Wolpert, 1998; Tanaka *et al.*, 2006). The central idea of these models is that the nervous system acts as a stochastically optimal controller, i.e. a controller which plans optimal movements taking the statistics of noise (SDN_m) into account (review in Todorov, 2004). The scaling law results from time minimization while attempting to reach a target area: due to noise, for each amplitude, there is a unique (minimum) movement duration which guarantees that movement endpoint is bounded to a given spatial region. Speed/accuracy trade-off is a consequence of SDN_m: faster movements require larger control signals, and thus endure more noise. On this basis, the models predict that movement duration is not simply a function of amplitude and target width, but especially of the ratio between amplitude and target width (Eq. 8).

The weakness of these models is the absence of online feedback control which is necessary

for the continuous updating of motor commands by internal and external feedback loops (Desmurget & Grafton, 2000; Todorov & Jordan, 2002; Saunders & Knill, 2004; Guigon *et al.*, 2008). Thus we tried to reproduce Fitts' law in the framework of optimal feedback control. We simulated visually-guided movements (see **Materials and Methods**) of different amplitudes and durations under SDN_m, and we measured the terminal variability (Ω). Then we searched for pairs (A,MT) which lead to a given W (i.e. $\Omega = W$). We repeated this operation for different values of W, and we plotted MT as a function of $\log_2(2A/W)$ (Fig. 4*A*). It appears clearly that MT is a function of A/W as required by Eq. 8. Similar results were obtained in the presence of delay in sensory feedback ($\Delta = 100$ ms; Fig. 4*A*, *gray lines*). We reproduced similar simulations for nonvisually guided-movements (see **Materials and Methods**). The data obviously deviated from Fitts' law (Fig. 4*B*).

We addressed the influence of the exponent of noise for SDN_m. We reproduced the simulations of Fig. 4*A* for $p = 1.5$ (Fig. 4*A*, *dashed lines*). Clearly, the data deviated from Fitts' law. A similar result was reported by Iguichi *et al.* (2005) with the minimim variance model (their Fig. 9).

For Fitts' law, amplitude/duration scaling can arise as a consequence of a constant variability criterion (see Harris & Wolpert, 1998; Tanaka *et al.*, 2006; and above). However, scaling is also found in the absence of Fitts' law, e.g. when subjects reach for visual targets with no constraints of accuracy. In this case, scaling is associated with a pattern of amplitude-dependent variability (Gordon *et al.*, 1994a; Messier & Kalaska, 1997, 1999; van Beers *et al.*, 2004). We have shown previously that scaling can result from a constant effort criterion (Guigon *et al.*, 2007, 2008). Interestingly, in the absence of sensory noise (visual feedback condition), effort and variability are univocally related (Fig. 4*C*). Thus Fitts' law could ensue from a constant effort criterion. In the presence of proprioceptive noise (nonvisual feedback condition), there is

no longer a one-to-one relationship between effort and variability (Fig. 2*D*), and scaling based on constant effort can be associated with non constant variability (see below). The question turns to the nature of noise in proprioceptive feedback.

Evidence for noise in proprioceptive feedback

The structure of motor variability (i.e. how variability changes in time and space along a movement) reveals critical information on motor control processes and the nature of noises that corrupt these processes (Harris & Wolpert, 1998; Todorov & Jordan, 2002; van Beers *et al.*, 2004; Guigon *et al.*, 2008). For instance, the variability of radially pointing movements has revealed that several types of noise, not only SDN_m, are present in the motor system (van Beers *et al.*, 2004). This conclusion was reached using an open-loop model which is not appropriate to evaluate the influence of feedback noise. Thus we assessed the influence of sensory and motor noise on the variability of radially pointing movements using optimal feedback control. We were interested in the shape and orientation of endpoint distributions for movements of the unseen limb (variability ellipses; Fig. 3*B*, inset; Gordon *et al.*, 1994a; Messier & Kalaska, 1997, 1999; van Beers *et al.*, 2004). As the shape and orientation of variability ellipses appear to depend on limb inertia (van Beers *et al.*, 2004), we simulated an inertial point in two-dimensional space with different masses in two orthogonal directions (see **Materials and Methods**).

We first simulated nonvisually-guided movements in a single direction (45 deg) to explore the influence of different types of noise in a systematic fashion. We observed that the surface area, shape, and orientation of ellipses were mostly determined by signal-dependent sensory noise (SDN_s) while signal-independent sensory noise (SIN_s) contributed basically to their surface area (Fig. 5*A*,*B*). Motor noise (SDN_m, SIN_m) had little influence. We found that variability ellipse was elongated for both SDN_m and SDN_s (Fig. 3*A*,*B*), but aligned along

movement direction only for SDN_s (Fig. 5*B*). This result was confirmed by a quantitative analysis (Fig. 5*A*,*B*). On the one hand, ellipse orientation was almost constant under SDN_m and deviated from movement direction by >45° (Fig. 5*A*). On the other hand, orientation tended to be closer to movement direction as SDN_s increased (*orientation effect*; Fig. 5*B*).

Then, we simulated movements in 5 directions in the first quadrant (because system dynamics is invariant by horizontal and vertical symmetry). Under SDN_m, the variability ellipses had an almost constant orientation, irrespective of movement direction (Fig. 6*A*). In contrast, the ellipses were closely aligned on movement direction under SDN_s (Fig. 6*B*). These results are confirmed by a polar plot (*left* in Fig. 6*C*,*D*). We further observed that the aspect ratio varies with movement direction under SDN_s, but less under SDN_m (*center* in Fig. 6*C*,*D*). Ellipse surface area was constant across directions under SDN_m, but varied with direction under SDN_s (*right* in Fig. 6*C*,*D*). The results in Fig. 6*D* closely match experimental observations reported in van Beers *et al.* (2004) (see also Desmurget *et al.*, 1997; Gepshtein *et al.*, 2007). A main effect was the variation of aspect ratio with movement direction. In the model, the ratio was higher in directions of smaller inertia, i.e. 90/270°. In van Beers *et al.* (2004), the directions were ~60/250° (their Fig. 4*A*). Although initial arm posture is not known exactly for the data of van Beers *et al.* (2004), these directions likely correspond to movements obtained by forearm rotations, i.e. movements against smaller inertial loads (Gordon *et al.*, 1994b).

Influence of feedback delay was assessed separately (Fig. 7). We observed that the delay had a weak influence on the shape of variability ellipses (Fig. 7*A*), but a strong influence on their size (Fig. 7*B*). The orientation effect decreased with the delay, but remained visible even at the longer delay (Fig. 7*C*).

Although these results are consistent with experimental observations, it is not easy to justify that the behavior of an articulated arm can be adequately represented by the behavior of an

inertial point. Thus we addressed the results obtained with the simple linear model (Fig. 6) using an optimal feedback control model for a planar two-joint arm (see **Materials and Methods**). The results are shown in Fig. 8*A*,*B*, in the same format as in Fig. 6C,*D*. Although the results are less striking than in the linear case, we observed a similar trend as with the linear model, i.e. ellipse orientation became aligned with movement direction in the presence of SDN_S. Two interesting characteristics are the anisotropic variations of aspect ratio and surface area with movement direction (Fig. 8*B*, *center* and *right*). Using principal component analysis, we calculated the orientation of the main axis of these variations (61° for aspect ratio, 23° for surface area; *gray lines* in Fig. 8*B*). For comparison, we estimated these quantities for the experimental results of van Beers *et al.* (2004) (their Fig. 4*A*,*C*): we found 60° and 28° for the aspect ratio and the surface area, respectively (*dashed lines* in Fig. 8*B*). Although the nonlinear model reproduces quantitative features of experimental data, it does not reproduce the actual size of variability ellipses. With our parameters (size of noises), maximum surface area was 2.2 cm^2 (we observed that larger noises lead to unrealistic trajectories and velocity profiles), whereas it could be 5-10 cm^2 for real movements (Fig. 3 in van Beers *et al.*, 2004). A possible reason for this discrepancy is the absence of feedback delay in the nonlinear model. We have shown in the linear model that the delay increases the size of variability ellipses, but has little influence on their shape and orientation (Fig. 7). This property could be true for the nonlinear model, but to prove it is a challenging problem of computing power (see **Materials and Methods**).

Since nonlinear modeling is a complex problem, these simulations should be considered with caution. Yet they point to a critical contribution of signal-dependent noise in proprioceptive feedback to motor variability when subjects do not receive specific instruction regarding movement accuracy. This case is complementary to the condition of Fitts' law which requires

perfect sensory feedback (see above).

These results suggest that the structure of variability of reaching movements can be quantitatively explained by the interplay between signal-dependent proprioceptive and motor noises in an optimal feedback controller. We now address the control of movement accuracy.

Control of accuracy

Experimental studies have shown that subjects can be trained to produce a desired kinematic pattern (velocity profile) while modulating terminal accuracy (Gribble *et al.*, 2003; Osu *et al.*, 2004). A central observation was that movement accuracy covaried positively with the level of muscular cocontraction despite the fact that the variability of motor patterns (EMGs and torques) increased with cocontraction. We explored this paradox with the model. On the one hand, we have shown that movement variability related to control of accuracy can be explained by a reduced influence of proprioceptive noise. On the other hand, cocontraction should increase motor noise. Thus we assessed the effect of opposite variations in proprioceptive and motor noises (nonvisually-guided movements) as a simplified way to address the influence of cocontraction. We compared two conditions: 1. "normal cocontraction" ($\sigma_{SDNm} = 0.7$ and $\sigma_{SDNs} = 0.2$); 2. "high cocontraction" ($\sigma_{SDNm} = 0.8$ and $\sigma_{SDNs} = 0.1$). We observed that, for this particular choice of noise, movement was more accurate in the high cocontraction condition (Fig. 9*A*,*B*), although the forces and EMGs were more variable in this condition (Fig. 9*D*,*E*; see Fig. 5 in Osu *et al.*, 2004). We also note that higher cocontraction lead to larger variability over ~3/4 of the trajectory (Fig. 9*C*; see Fig. 5*G* in Osu *et al.*, 2004, Fig. 5*C* in Selen *et al.*, 2006). These results were obtained for a specific combination of proprioceptive and motor noise, but remain similar for many different combinations. As we varied σ_{SDNm} and σ_{SDNs} in the range 0.1-0.7 , we observed that for a 20% increase in σ_{SDNm}, a 50% decrease in σ_{SDNs} was in general

appropriate to produce a "cocontraction effect" (i.e. the movement was more precise while the forces and EMG were more variable). The main significance of these results is that we were able to account quantitatively for the influence of cocontraction using the same components as used to explain the characteristics of variability ellipses. The model illustrates the possible effect of opposite modulation of sensory and motor noises, but does not reveal a principle for their coordinated variations. We also calculated the spatial variability of distance to kinematic landmarks (peak acceleration, velocity and deceleration; Fig. 9*F*). We observed that the variability increased until peak deceleration and then plateaued in the first condition. The variability decreased after peak deceleration in the second condition (lower SDN_s). This result was still more marked for $SDN_s = 0$, corresponding to the case of a visually guided movement. This observation is consistent with experimental observations (Fig. 9 in Proteau & Isabelle, 2002; Fig. 4 in Khan & Franks, 2003; Fig. 1 in Khan *et al.*, 2003). Similar results were obtained for nonzero feedback delay.

Analysis of parameters (linear model)

A central emerging effect of the model is the influence of SDN_s on the orientation of variability ellipses (Fig. 6*D*). Here, we address the influence of different parameters on this effect.

Observation matrix

We assessed how the structure of the observation matrix influenced the orientation effect. Accordingly we selectively removed the position (P), velocity (V), activation (A) and excitation (E) information from the observation matrix (e.g. the combination PV means that only position and velocity were observable). We found that the orientation effect was present for a majority of combinations of observable states although no simple rule could be drawn. Exceptions were the following combinations of observable states: PVE, PE, VE, E.

Structure of signal-dependent sensory noise

The orientation effect was completely suppressed in the case of independent sources of noise (d = 8), but was not improved by the presence of a unique source of noise (d = 1). It is possible that the orientation effect could emerge under weaker hypotheses on the structure of noise. However, a finer analysis of this issue would not be necessarily meaningful in the framework of our simplified model.

Discussion

There are three main results in this study. First, we have shown that the structure of variability of nonvisually-guided reaching movements can be quantitatively explained by the interplay between signal-dependent proprioceptive and motor noises in an optimal feedback controller. Second, the variability of movement performed under a constraint of accuracy (e.g. condition of Fitts' law) reflects optimal feedback control in the presence of perfect sensory feedback. Third, the surplus of motor noise and the resulting increase in motor output variability related to increased muscular cocontraction is not incompatible with improved terminal accuracy.

Nature of the model

The present model was cast in the framework of linear dynamical systems (for a similar approach, see Todorov & Jordan, 2002; Saunders & Knill, 2004). This simplification lead to an analytically tractable problem which can be easily solved in the presence of noise. Such a linear model was found appropriate to address general characteristics of motor variability (Harris & Wolpert, 1998; Todorov & Jordan, 2002; Saunders & Knill, 2004; Tanaka *et al.*, 2006; present results). For instance, Fitts' law has been observed in a wide range of conditions (Plamondon & Alimi, 1997), including mentally simulated movements (Decety & Jeannerod, 1995). A

linear approach can be suitable in this case. However, it was unclear whether the linear framework is also suitable to address aspects of variability which likely depend on nonlinearities in motor behavior, e.g. direction-dependent changes in the shape of terminal variability ellipses in reaching movements (Gordon *et al.*, 1994a; van Beers *et al.*, 2004). Thus, we also simulated a more realistic nonlinear model (a planar articulated arm actuated by two pairs of antagonist muscles) to address this issue.

The proposed model is a computational approach to motor control and variability. It is not a model of physiological mechanisms involved in motor control. Thus we considered the general case of noise in sensory and motor pathways, and as an approximation, we considered signal-independent and signal-dependent noises (Todorov, 2005). We found that a computational description of terminal variability can be obtained by the presence of signal-dependent noise in sensory pathways. Yet, we do not claim that there is SDN at the level of muscle spindles or Golgi tendon organs, but the model predicts that there is some form a SDN in sensory pathways (somewhere between the sensors and the state estimator).

Structure of motor variability for reaching movements

Although it is well recognized that variability of goal-directed movements derives in part from the presence of noise in the execution process (Hoff & Arbib, 1993; Harris & Wolpert, 1998; Messier & Kalaska, 1999; Todorov & Jordan, 2002; van Beers *et al.*, 2004), the nature of noise remains poorly understood. Theoretical studies have shown that part of the noise is signal-dependent motor noise, as this type of noise appears necessary for the emergence of raw aspects of structured variability, e.g. uncontrolled manifolds which are found in line-pointing and via-point tasks (Todorov & Jordan, 2002; Guigon *et al.*, 2008). Yet, SDN_m is not sufficient to account for the spatio-temporal variability of reaching movements (van Beers *et al.*, 2004; present results). For instance, the ubiquitous finding that directional errors are smaller than

errors in amplitude (Gordon *et al.*, 1994a; Messier & Kalaska, 1997, 1999; van Beers *et al.*, 2004) cannot be reproduced with SDN_m. van Beers *et al.* (2004) proposed that execution is corrupted by a mixture of constant noise, temporal noise and SDN_m. However, their account of experimental data was not fully conclusive since they used an open-loop control model.

Our model suggests that noise in proprioceptive feedback is an important determinant of the variability of nonvisually-guided reaching movements. It should be noted that this noise is not of a different nature than motor noise. In fact, both types of noise are signal-dependent, which means that their variance increases proportionally to the magnitude of the signal. The sole difference is the nature of the neural pathway (sensory or motor) in which the signal flows.

Fitts' law

Although there is no consensus on the origin of Fitts' law (e.g. Plamondon & Alimi, 1997), the idea has grown that it could ensue from the attempt to control movement accuracy in the presence of SDN_m (Meyer *et al.*, 1988; Harris & Wolpert, 1998; Tanaka *et al.*, 2006). This idea is especially interesting as it also provides a principled approach to the emergence of motor behaviors (Harris & Wolpert, 1998). However, there are three main limitations of the minimum variance model. First it is an open loop model which fails to exploit feedback processing (Todorov & Jordan, 2002; Guigon *et al.*, 2008). Second, it is bound to exhibit speed/accuracy trade-off (i.e. faster movements are necessarily more variable), and thus it cannot account for the paradoxical effect of cocontraction (see **Control of accuracy** below). Third, the choice of a terminal variance can be problematic in more than one dimension since the shape of the variance area has to be specified. For instance, it has been shown with pointing movements that the shape of the variance area is not identical to the shape of the target region (Osu *et al.*, 2004; Gepshtein *et al.*, 2007).

To circumvent these difficulties, we attempted to extend the results obtained with the

minimum variance model in the framework of feedback control. This extension was successful, and adds support and sense to the contention of Harris and Wolpert. Fitts' law holds empirically when subjects are instructed to perform accurately, and in the model when sensory feedback is perfect. This situation corresponds to the case where the influence of proprioception is reduced in the presence of vision due their relative variabilities and the functioning of the Kalman filter. We can make the reasonable proposal that accuracy can be better controlled if the influence of proprioceptive feedback is reduced in the presence of visual feedback. This view is consistent with experimental observations. The fact that movements are more accurate in the presence than in the absence of visual feedback of the moving limb (Woodworth, 1899) can be related to the generally greater precision of vision over proprioception. In the absence of vision, subjects do not scale their variability to the size of the target (Chua & Elliott, 1993).

An ubiquitous property of motor control is amplitude/duration scaling, i.e. movements of larger amplitude last longer. According to the model, this property arises from a constant effort principle (Guigon *et al.*, 2007, 2008): if movements of different amplitudes are realized with the same level of effort, their duration should increase with their amplitude. This principle provides a general account of scaling. In the absence of sensory noise, effort and variability covary and the constant effort principle generates a scaling which conforms to Fitts' law. In the presence of sensory noise, scaling also occurs, but the pattern of variability is dictated by the structure of noise. Thus, the present model relieves the three difficulties of the minimum variance model (see also **Control of accuracy** below).

An interesting issue is the kinematic characteristics of aiming trajectories under Fitts' law. Amplitude and target width exert different effects on movement kinematics (Soechting, 1984; MacKenzie *et al.*, 1987; Marteniuk *et al.*, 1987). Although the two parameters influence movement time, amplitude primarily determines acceleration duration and peak velocity while

target width has almost no effect on acceleration duration and peak velocity, but affects the duration of the deceleration phase. The classical interpretation of these observations is based on Woodworth's initial adjustment and current control phases, i.e. an initial quick ("ballistic") transport toward target location followed by a slower feedback-driven homing phase. In its current form, the model does not provide a direct explanation of these results. In fact, the central issue is how target size is exploited by the controller. Target size could be used to specify boundary conditions, e.g. where the controlled system should land within the target area. However, in the presence of noise, there is no guarantee that the actual landing point will be within the required region. A more efficient solution would consist in matching target size and "effective target width", i.e. searching for a control law which, taking into account the expected characteristics of noise and feedback, would produce an actual endpoint dispersion corresponding to the target region. The constant effort principle could be modified to encompass this idea. Reprogramming at each time would lead to adjust remaining duration not only as a function of remaining amplitude and remaining effort, but also as a function of a desired final variability. The scenario could be the following. Before the arrival of sensory feedback, the controller is driven by target distance and a level of effort. Once feedback is available, the controller can exploit characteristics of the feedback to improve the motor plan. For instance, feedback of visual origin could allow accuracy control. At this stage, target size can be introduced in the plan: remaining movement duration is updated in such a way that predictable final variability matches target size. This updating is rather simple since variability and effort are univocally related. A consequence is that the duration of the later part of the movement should scale with target size. It should be noted that the movement was divided in two parts for simplicity, but in fact no real division exists since feedback is continuous.

Control of accuracy

Motor variability has been generally ascribed to the presence of signal-dependent noise in motor signals (Meyer *et al.*, 1988; Harris & Wolpert, 1998; Todorov & Jordan, 2002; van Beers *et al.*, 2004). This hypothesis lead ineluctably to speed/accuracy trade-off. However, it is widely recognized that not all motor behaviors conform to such a trade-off. The process of learning a new motor task results in movements which are both faster and less variable (Darling *et al.*, 1988; Corcos *et al.*, 1993; Jaric *et al.*, 1994; Ilic *et al.*, 1996; Jaric & Latash, 1999; Gabriel, 2002; Domkin, 2005). For instance, subjects can be trained to modulate terminal accuracy while preserving a common kinematic pattern (Gribble *et al.*, 2003; Osu *et al.*, 2004). The model shows that these paradoxical observations can be assigned to the functioning of the state estimator. It is logical that a more precise estimate should allow a better programming and a more consistent performance. However, a less intuitive aspect is that improved performance is not a simple consequence of a global reduction of uncertainty in the motor system, but can coincide with a greater variability in motor commands. In fact, feedback control can exploit covariation among motor outputs to reduce task variability (Müller & Sternad, 2004). Accordingly, there is no fundamental contradiction between cocontraction, which likely increases motor variability (Osu *et al.*, 2004), and accuracy (van Galen & Schomaker, 1992; van Gemmert & van Galen, 1997; Laursen *et al.*, 1998; van Galen & van Huygevoort, 2000; Gribble *et al.*, 2003; Osu *et al.*, 2004; Sandfeld & Jensen, 2005; van Roon *et al.*, 2005).

Yet the question remains of the mechanism, which links cocontraction and accuracy. A possible mechanism is based on modulation of impedance. Muscle cocontraction can increase joint stiffness (Hogan, 1984; Al-Falahe & Vallbo, 1988; De Serres & Milner, 1991; Osu & Gomi, 1999), and allows the limb to counteract disturbances and instabilities (De Serres & Milner, 1991; Burdet *et al.*, 2001; Franklin *et al.*, 2004; Milner, 2004), which could be liable

for a better accuracy (Burdet *et al.*, 2001; Shiller *et al.*, 2002). For this scenario to be applicable, it should be hypothesized that there exists at each time an "operating" point which corresponds to the unperturbed trajectory, and which is used to measure and apply elastic restoring forces. This hypothesis is in theory applicable to models which exploit the tracking of a reference trajectory, e.g. equilibrium-point models (Flanagan *et al.*, 1993; Gribble *et al.*, 1998) and models based on combined inverse dynamics and impedance control (Franklin *et al.*, 2003; Osu *et al.*, 2003). Two models have addressed this issue. van Galen & de Jong (1995) have shown that a mass attached to a spring is more accurately controlled in the presence of motor noise when the level of static forces is higher. However, control of accuracy in this model results from a restoring force toward a fixed point, which makes little functional sense. Selen *et al.* (2005) reached a similar conclusion for the control around an equilibrium point, but it is unclear whether the model can be extended to movements governed by a moving equilibrium point. In our model, there is no reference trajectory, but the operating point could be the currently estimated position of the limb since this point is maintained as the equilibrium point of static forces applied to the limb (separation principle; see Guigon *et al.*, 2007a for a discussion). In this case, modulation of impedance could contribute to stability, but not directly to accuracy since impedance has no direct influence on the efficiency of the state estimator, i.e. it will not compensate for a wrong operating point.

An alternative hypothesis to relate cocontraction and accuracy is based on the notion of fusimotor control, i.e. the central modulation of the sensitivity of muscles spindles. It is well documented that fusimotor activity is stronger for tasks requiring greater attention or precision (Prochazka, 1989; Hulliger, 1993; Kakuda *et al.*, 1996; Nafati *et al.*, 2004). Since co-activation of skeletomotor and fusimotor systems seems to be the rule in humans (Vallbo *et al.*, 1979; Kakuda *et al.*, 1996; Gandevia *et al.*, 1997), a likely consequence of increased fusimotor control

is increased muscular cocontraction. The question remains of the mechanism by which fusimotor activity contributes to accuracy of movement. A general proposal is that fusimotor control would act to optimize the transmission of sensory feedback information (Loeb & Marks, 1985; Loeb *et al.*, 1985; Loeb *et al.*, 1999). In particular, there is evidence that the gamma system can enhance information transmission from populations of muscle spindles (Milgram & Inbar, 1976; Inbar *et al.*, 1979; Bergenheim *et al.*, 1995, 1996; Tock *et al.*, 2005). This is true despite the fact that signal from individual spindles are more variable under γ stimulation (Bergenheim *et al.*, 1995). We note that this variability is consistent with the presence of signal-dependent noise in sensory feedback since a basic effect of fusimotor input is to increase the mean discharge rate of spindles (Hulliger *et al.*, 1977).

We note that this article is concerned with temporary improvement in movement accuracy. In this framework, the speed/accuracy paradox is explained by the effect of muscular cocontraction. This view is consistent with the presence of concontraction during early phases of learning of a novel task (Person 1958; Milner & Cloutier, 1993; Thoroughman & Shadmher, 1999; Osu *et al.*, 2002). We did not address mechanisms involved in long-term changes in accuracy.

Significance of the results

We have shown that the speed/accuracy paradox for reaching movements can be explained by the joint influence exerted by sensory and motor signal-dependent noises during motor execution. This result is all the more interesting because the same types of noise appear to shape the characteristics of variability ellipses of reaching movements. More generally, the present model provides a principled framework to the study of motor variability which is more versatile than previous approaches (Harris & Wolpert, 1998; Todorov & Jordan, 2002).

References

Al-Falahe, N.A. & Vallbo, A.B. (1988) Role of the human fusimotor system in a motor adaptation task. *J. Physiol. (Lond.)*, **401**, 77-95.

Baddeley, R.J., Ingram, H.A. & Miall, R.C. (2003) System identification applied to a visuomotor task: Near-optimal human performance in a noisy changing task. *J. Neurosci.*, **23**, 3066-3675.

Bergenheim, M., Johansson, H. & Pedersen, J. (1995) The role of the gamma-system for improving information transmission in populations of Ia afferents. *Neurosci. Res.*, **23**, 207-215.

Bergenheim, M., Johansson, H., Pedersen, J., Ohberg, F. & Sjolander, P. (1996) Ensemble coding of muscle stretches in afferent populations containing different types of muscle afferents. *Brain Res.*, **734**, 157-166.

Bevington, P.R. (1969) *Data reduction and error analysis for the physical sciences*. McGraw-Hill Book Company, New York.

Burdet, E., Osu, R., Franklin, D.W., Milner, T.E. & Kawato, M. (2001) The central nervous system stabilizes unstable dynamics by learning optimal impedance. *Nature*, **414**, 446-449.

Christou, E.A. & Carlton, L.G. (2002) Age and contraction type influence motor output variability in rapid discrete tasks. *J. Appl. Physiol.*, **93**, 489-498.

Chua, R. & Elliott, D. (1993) Visual regulation of target-directed movements. *Hum. Mov. Sci.*, **12**, 365-401.

Churchland, M.M., Afshar, A. & Shenoy, K.V. (2006) A central source of movement variability. *Neuron*, **52**, 1085-1096.

Corcos, D.M., Jaric, S., Agarwal, G.C. & Gottlieb, G.L. (1993) Principles for learning single-joint movements. I. Enhanced performance by practice. *Exp. Brain Res.*, **94**, 499-513.

Darling, W.G., Cole, K.J. & Abbs, J.H. (1988) Kinematic variability of grasp movements as a function of practice and movement speed. *Exp. Brain Res.*, **73**, 225-235.

De Serres, S.J. & Milner, T.E. (1991) Wrist muscle activation patterns and stiffness associated with stable and unstable mechanical loads. *Exp. Brain Res.*, **86**, 451-458.

Desmurget, M. & Grafton, S. (2000) Forward modeling allows feedback control for fast reaching movements. *Trends Cogn. Sci.*, **4**, 423-431.

Desmurget, M., Jordan, M.I., Prablanc, C. & Jeannerod, M. (1997) Constrained and unconstrained movements involve different control strategies. *J. Neurophysiol.*, **77**, 1644-1650.

Domkin, D. (2005) *Perception and control of upper limb movement: Insights gained by analysis of sensory and motor variability*. Unpublished doctoral dissertation, Umea University, Umea, Sweden.

Fitts, P.M. (1954) The information capacity of the human motor system in controlling the amplitude of movement. *J. Exp. Psychol.*, **47**, 381-391.

Flanagan, J.R., Ostry, D.J. & Feldman, A.G. (1993) Control of trajectory modifications in target-directed reaching. *J. Mot. Behav.*, **25**, 140-152.

Franklin, D.W., Osu, R., Burdet, E., Kawato, M. & Milner, T.E. (2003) Adaptation to stable and unstable dynamics achieved by combined impedance control and inverse dynamics model. *J. Neurophysiol.*, **90**, 3270-3282.

Franklin, D.W., So, U., Kawato, M. & Milner, T.E. (2004) Impedance control balances stability with metabolically costly muscle activation. *J. Neurophysiol.*, **92**, 3097-3105.

Gabriel, D.A. (2002) Changes in kinematic and EMG variability while practicing a maximal performance task. *J. Electromyogr. Kinesiol.*, **12**, 407-412.

Gandevia, S.C., Wilson, L.R., Inglis, J.T. & Burke, D.A. (1997) Mental rehearsal of motor tasks recruits alpha-motoneurones but fails to recruit human fusimotor neurones selectively. *J.*

Physiol. (Lond.), **505**, 259-266.

Gepshtein, S., Seydell, A. & Trommershäuser, J. (2007) Optimality of human movement under natural variations of visual-motor uncertainty. *J. Vis.*, **7**, 1-18.

Ghahramani, Z., Wolpert, D.M. & Jordan, M.I. (1996) Generalization to local remappings of the visuomotor coordinate transformation. *J. Neurosci.*, **16**, 7085-7096.

Gordon, J., Ghilardi, M.F. & Ghez, C. (1994a) Accuracy of planar reaching movements. I. Independence of direction and extent variability. *Exp. Brain Res.*, **99**, 97-111.

Gordon, J., Ghilardi, M.F., Cooper, S.E. & Ghez, C. (1994b) Accuracy of planar reaching movements. II. Systematic extent errors resulting from inertial anisotropy. *Exp. Brain Res.*, **99**, 112-130.

Gribble, P.L., Mullin, L.I., Cothros, N. & Mattar, A. (2003) Role of cocontraction in arm movement accuracy. *J. Neurophysiol.*, **89**, 2396-2405.

Gribble, P.L., Ostry, D.J., Sanguineti, V. & Laboissière, R. (1998) Are complex control signals required for human arm movement? *J. Neurophysiol.*, **79**, 1409-1424.

Guigon, E., Baraduc, P. & Desmurget, M. (2007a) Computational motor control: Redundancy and invariance. *J. Neurophysiol.*, **97**, 331-347.

Guigon, E., Baraduc, P. & Desmurget, M. (2007b) Coding of movement- and force-related information in primate primary motor cortex: A computational approach. *Eur. J. Neurosci.*, **26**, 250-260.

Guigon, E., Baraduc, P. & Desmurget, M. (2008) Optimality, stochasticity, and variability in motor behavior. *J. Comput. Neurosci.*, in press.

[http://e.guigon.free.fr/optimality.pdf]

Harris, C.M. & Wolpert, D.M. (1998) Signal-dependent noise determines motor planning. *Nature*, **394**, 780-784.

Hoff, B. & Arbib, M.A. (1993) Models of trajectory formation and temporal interaction of reach

and grasp. *J. Mot. Behav.*, **25**, 175-192.

Hogan, N. (1984) Adaptive control of mechanical impedance by coactivation of antagonist muscles. *I.E.E.E. Trans. Automat. Control*, **AC-29**, 681-690.

Hogan, N. (1985) The mechanics of multi-joints postures and movement. *Biol. Cybern.*, **52**, 315-331.

Hulliger, M. (1993) Fusimotor control of proprioceptive feedback during locomotion and balancing: Can simple lessons be learned for artificial control of gait? *Prog. Brain Res.*, **97**, 173-180.

Hulliger, M., Matthews, P.B. & Noth, J. (1977) Static and dynamic fusimotor action on the response of Ia fibres to low frequency sinusoidal stretching of widely ranging amplitude. *J. Physiol. (Lond.)*, **267**, 811-838.

Iguchi, N., Sakaguchi, Y. & Ishida, F. (2005) The minimum endpoint variance trajectory depends on the profile of the signal-dependent noise. *Biol. Cybern.*, **92**, 219-228.

Ilic, D.B., Corcos, D.M., Gottlieb, G.L., Latash, M.L. & Jaric, S. (1996) The effects of practice on movement reproduction: Implications for models of motor control. *Hum. Mov. Sci.*, **15**, 101-114.

Inbar, G.F., Madrid, J. & Rudomin, P. (1979) The influence of the gamma system on cross-correlated activity of Ia spindles and its relation to information transmission. *Neurosci. Lett.*, **13**, 73-78.

Jaric, S., Corcos, D.M., Gottlieb, G.L., Ilic, D.B. & Latash, M.L. (1994) The effects of practice on movement distance and final position reproduction: Implications for the equilibrium-point control of movements. *Exp. Brain Res.*, **100**, 353-359.

Jaric, S. & Latash, M.L. (1999) Learning a pointing task with a kinematically redundant limb: Emerging synergies and patterns of final position variability. *Hum. Mov. Sci.*, **18**, 819-838.

Jones, K.E., Hamilton, A.F. & Wolpert, D.M. (2002) Sources of signal-dependent noise during

isometric force production. *J. Neurophysiol.*, **88**, 1533-1544.

Kakuda, N., Vallbo, A.B. & Wessberg, J. (1996) Fusimotor and skeletomotor activities are increased with precision finger movement in man. *J. Physiol. (Lond.)*, **492**, 921-929.

Kerr, G.K. & Worringham, C.J. (2002) Velocity perception and proprioception. *Adv. Exp. Med. Biol.*, **508**, 79-86.

Khan, M.A. & Franks, I.M. (2003) Online versus offline processing of visual feedback in the production of component submovements. *J. Mot. Behav.*, **35**, 285-295.

Khan, M.A., Lawrence, G., Fourkas, A., Franks, I.M., Elliott, D. & Pembroke, S. (2003) Online versus offline processing of visual feedback in the control of movement amplitude. *Acta Psychol. (Amst.)*, **113**, 83-97.

Laidlaw, D.H., Bilodeau, M. & Enoka, R.M. (2000) Steadiness is reduced and motor unit discharge is more variable in old adults. *Muscle & Nerve*, **23**, 600-612.

Laursen, B., Jensen, B.R. & Sjøgaard, G. (1998) Effect of speed and precision demands on human shoulder muscle electromyography during a repetitive task. *Eur. J. Appl. Physiol. Occup. Physiol.*, **78**, 544-548.

Loeb, G.E., Brown, I.E. & Cheng, E.J. (1999) A hierarchical foundation for models of sensorimotor control. *Exp. Brain Res.*, **126**, 1-18.

Loeb, G.E., Hoffer, J.A. & Marks, W.B. (1985) Activity of spindle afferents from cat anterior thigh muscles. III. Effects of external stimuli. *J. Neurophysiol.*, **54**, 578-591.

Loeb, G.E. & Marks, W.B. (1985) Optimal control principles for sensory transducers. In Boyd, I.A. & Gladden, M.H., (eds) *Proc International Symposium: the muscle spindle*. MacMillan Ltd, London, pp. 409-415.

MacKenzie, C.L., Marteniuk, R.G., Dugas, C., Liske, D. & Eckmeier, B. (1987) Three dimensional movement trajectories in Fitts' task: Implications for control. *Q. J. Exp. Psychol. A*, **39**, 629-647.

Marteniuk, R.G., MacKenzie, C.L., Jeannerod, M., Athenes, S. & Dugas, C. (1987) Constraints on human arm movement trajectories. *Can. J. Psychol.*, **41**, 365-378.

McIntyre, J., Stratta, F. & Lacquaniti, F. (1997) Viewer-centered frame of reference for pointing to memorized targets in three-dimensional space. *J. Neurophysiol.*, **78**, 1601-1618.

Messier, J. & Kalaska, J.F. (1997) Differential effect of task conditions on errors of direction and extent of reaching movements. *Exp. Brain Res.*, **115**, 469-478.

Messier, J. & Kalaska, J.F. (1999) Comparison of variability of initial kinematics and endpoints of reaching movements. *Exp. Brain Res.*, **125**, 139-152.

Meyer, D.E., Abrams, R.A., Kornblum, S., Wright, C.E. & Smith, J.E.K. (1988) Optimality in human motor performance: Ideal control of rapid aimed movement. *Psychol. Rev.*, **95**, 340-370.

Milgram, P. & Inbar, G.F. (1976) Distortion suppression in neuromuscular information transmission due to interchannel dispersion in muscle spindles firing thresholds. *I.E.E.E. Trans. Biomed. Eng.*, **23**, 1-15.

Milner, T.E. (2004) Accuracy of internal dynamics models in limb movements depends on stability. *Exp. Brain Res.*, **159**, 172-184.

Milner, T.E. & Cloutier, C. (1993) Compensation for mechanically unstable loading in voluntary wrist movements. *Exp. Brain Res.*, **94**, 522-532.

Müller, H. & Sternad, D. (2004) Decomposition of variability in the execution of goal-oriented tasks: Three components of skill improvement. *J. Exp. Psychol.: Hum. Percept. Perform.*, **30**, 212-233.

Nafati, G., Rossi-Durand, C. & Schmied, A. (2004) Proprioceptive control of human wrist extensor motor units during an attention-demanding task. *Brain Res.*, **1018**, 208-220.

Osborne, L.C., Lisberger, S.G. & Bialek, W. (2005) A sensory source for motor variation. *Nature*, **437**, 412-416.

Osu, R., Burdet, E., Franklin, D.W., Milner, T.E. & Kawato, M. (2003) Different mechanisms involved in adaptation to stable and unstable dynamics. *J. Neurophysiol.*, **90**, 3255-3269.

Osu, R., Franklin, D.W., Kato, H., Gomi, H., Domen, K., Yoshioka, T. & Kawato, M. (2002) Short- and long-term changes in joint co-contraction associated with motor learning as revealed from surface EMG. *J. Neurophysiol.*, **88**, 991-1004.

Osu, R. & Gomi, H. (1999) Multijoint muscle regulation mechanisms examined by measured human arm stiffness and EMG signals. *J. Neurophysiol.*, **81**, 1458-1468.

Osu, R., Kamimura, N., Iwasaki, H., Nakano, E., Harris, C.M., Wada, Y. & Kawato, M. (2004) Optimal impedance control for task achievement in the presence of signal-dependent noise. *J. Neurophysiol.*, **92**, 1199-1215.

Person, R.S. (1958) Electromyographic investigations of coordination of the antagonistic muscles in development of motor habit. *Pavlov J. High Nerv. Act.*, **8**, 13-23.

Plamondon, R. & Alimi, A.M. (1997) Speed/accuracy trade-offs in target-directed movements. *Behav. Brain Sci.*, **20**, 279-349.

Prochazka, A. (1989) Sensorimotor gain control: A basic strategy of motor systems? *Prog. Neurobiol.*, **33**, 281-307.

Proteau, L. & Isabelle, G. (2002) On the role of visual afferent information for the control of aiming movements toward targets of different sizes. *J. Mot. Behav.*, **34**, 367-384.

Sandfeld, J. & Jensen, B.R. (2005) Effect of computer mouse gain and visual demand on mouse clicking performance and muscle activation in a young and elderly group of experienced computer users. *Appl. Ergon.*, **36**, 547-555.

Saunders, J.A. & Knill, D.C. (2004) Visual feedback control of hand movements. *J. Neurosci.*, **24**, 3223-3234.

Schmidt, R.A., Zelaznik, H.N., Hawkins, B., Franck, J.S. & Quinn, J.T. (1979) Motor-output variability: A theory for the accuracy of rapid motor acts. *Psychol. Rev.*, **86**, 415-451.

Scott, S.H. (2004) Optimal feedback control and the neural basis of volitional motor control. *Nat. Rev. Neurosci.*, **5**, 532-546.

Seidler-Dobrin, R.D., He, J. & Stelmach, G.E. (1998) Coactivation to reduce variability in the elderly. *Motor Control*, **2**, 314-330.

Selen, L.P., Beek, P.J. & van Dieën, J.H. (2005) Can co-activation reduce kinematic variability? A simulation study. *Biol. Cybern.*, **93**, 373-381.

Selen, L.P., Beek, P.J. & van Dieën, J.H. (2006) Impedance is modulated to meet accuracy demands during goal-directed arm movements. *Exp. Brain Res.*, **172**, 129-138.

Sergio, L.E. & Kalaska, J.F. (1998) Changes in the temporal pattern of primary motor cortex activity in a directional isometric force versus limb movement task. *J. Neurophysiol.*, **80**, 1577-1583.

Shiller, D.M., Laboissière, R. & Ostry, D.J. (2002) Relationship between jaw stiffness and kinematic variability in speech. *J. Neurophysiol.*, **88**, 2329-2340.

Soechting, J.F. (1984) Effect of target size on spatial and temporal characteristics of a pointing movement in man. *Exp. Brain Res.*, **54**, 121-132.

Sokal, R.R. & Rohlf, F.J. (1995) *Biometry: the principles and practice of statistics in biological research, 3rd ed*. W.H. Freeman, New York.

Stein, R.B., Gossen, E.R. & Jones, K.E. (2005) Neuronal variability: Noise or part of the signal? *Nat. Rev. Neurosci.*, **6**, 389-397.

Tanaka, H., Tai, M. & Qian, N. (2004) Different predictions by the minimum variance and minimum torque-change models on the skewness of movement velocity profiles. *Neural Comput.*, **16**, 2021-2040.

Tanaka, H., Krakauer, J.W. & Qian, N. (2006) An optimization principle for determining movement duration. *J. Neurophysiol.*, **95**, 3875-3886.

Thoroughman, K.A. & Shadmehr, R. (1999) Electromyographic correlates of learning an

internal model of reaching movements. *J. Neurosci.*, **19**, 8573-8588.

Tock, Y., Inbar, G.F., Steinberg, Y., Ljubisavljevic, M., Thunberg, J., Windhorst, U. & Johansson, H. (2005) Estimation of muscle spindle information rate by pattern matching and the effect of gamma system activity on parallel spindles. *Biol. Cybern.*, **92**, 316-332.

Todorov, E. (2002) Cosine tuning minimizes motor errors. *Neural Comput.*, **14**, 1233-1260.

Todorov, E. (2004) Optimality principles in sensorimotor controls. *Nat. Neurosci.*, **7**, 907-915.

Todorov, E. (2005) Stochastic optimal control and estimation methods adapted to the noise characteristics of the sensorimotor system. *Neural Comput.*, **17**, 1084-1108.

Todorov, E. & Jordan, M.I. (2002) Optimal feedback control as a theory of motor coordination. *Nat. Neurosci.*, **5**, 1226-1235.

Vallbo, A.B., Hagbarth, K.-E., Torebjörk, H.E. & Wallin, B.G. (1979) Somatosensory, proprioceptive, and sympathetic activity in human peripheral nerves. *Physiol. Rev.*, **59**, 919-957.

van Beers, R.J., Baraduc, P. & Wolpert, D.M. (2002) Role of uncertainty in sensorimotor control. *Philos. Trans. R. Soc. Lond. B Biol. Sci.*, **357**, 1137-1145.

van Beers, R.J., Haggard, P. & Wolpert, D.M. (2004) The role of execution noise in movement variability. *J. Neurophysiol.*, **91**, 1050-1063.

van Galen, G.P. & de Jong, W.P. (1995) Fitts' law as the outcome of a dynamic noise filtering model of motor control. *Hum. Mov. Sci.*, **14**, 539-571.

van Galen, G.P. & Schomaker, L.R.B. (1992) Fitts' law as a low-pass filter effect of muscle stiffness. *Hum. Mov. Sci.*, **11**, 11-21.

van Galen, G.P. & van Huygevoort, M. (2000) Error, stress and the role of neuromotor noise in space oriented behaviour. *Biol. Psychol.*, **51**, 151-171.

van Gemmert, A.W.A. & van Galen, G.P. (1997) Stress, neuromotor noise, and human performance: A theoretical perspective. *J. Exp. Psychol.: Hum. Percept. Perform.*, **23**, 1299-

1313.

van Roon, D., Steenbergen, B. & Meulenbroek, R.G. (2005) Trunk use and co-contraction in cerebral palsy as regulatory mechanisms for accuracy control. *Neuropsychologia*, **43**, 497-508.

Vindras, P. & Viviani, P. (1998) Frames of reference and control parameters in visuomanual pointing. *J. Exp. Psychol.: Hum. Percept. Perform.*, **24**, 569-591.

Visser, B., De Looze, M., De Graaff, M. & van Dieën, J. (2004) Effects of precision demands and mental pressure on muscle activation and hand forces in computer mouse tasks. *Ergonomics*, **47**, 202-217.

Wolpert, D.W. & Ghahramani, Z. (2000) Computational principles of movement neuroscience. *Nat. Neurosci.*, **3[Suppl]**, 1212-1217.

Woodworth, R.S. (1899) The accuracy of voluntary movement. *Psychol. Rev. Monogr.*, **3[Suppl2]**, 54-59.

Figure captions

Figure 1. *A*. An inertial point (*black square*) is driven by a noisy force $u(t)$. Its true position $x(t)$ is measured by a noisy sensor (ruler *at the top*; $y(t)$) which is used to define an estimated position $x\hat{}(t)$ (*dashed square*). Sources of noise are indicated by an *irregular arrow*. *B*. Trajectories of the inertial point. A particular trajectory ($x(t)$; *thick line*) is shown together with its corresponding estimated trajectory ($x\hat{}(t)$; *dashed line*).

Figure 2. Functioning of the model. A single time t is used for simplicity, but processing is in fact iterative. See Text for notations and details.

Figure 3. *A*. Simulated movements ($N = 500$) in direction 45° (10 cm, 400 ms) for SDN_m ($\sigma_{SDNm} = 0.5$). 20 endpoints and trajectories are shown. The 95% equal frequency ellipse is plotted. Ellipse orientation is 55.6°, aspect ratio is 1.38 and surface area is 1.29 cm^2 (see Inset in *B* for definitions). Scale bar = 2 cm. Parameters were: $\sigma_{SINm} = 0$, $\sigma_{SINs} = 0.06$, $\sigma_{SDNs} = 0.0$. Inset: 10 velocity profiles. *B*. Same as *A* for SDN_s ($\sigma_{SDNs} = 0.2$). Ellipse orientation is 5.6°, aspect ratio is 1.42 and surface area is 1.67 cm^2. Parameters: $\sigma_{SINm} = 0$, $\sigma_{SDNm} = 0.5$, $\sigma_{SINs} = 0.05$. Inset: ellipse orientation (θ) is the angle of the major axis of the ellipse relative to a reference direction (*arrow*), e.g. movement direction. Aspect ratio (ellipse elongation) is λ_1/λ_2. The quantities λ_1 and λ_2 ($\lambda_1 \geq \lambda_2$) are the square root of the eigenvalues of the covariance matrix of endpoint distribution. *C*. Control signal ($q_1(t)$) for a movement in *A*. The ideal control signal (zero noise; *black line*) and a real control signal (nonzero noise; *gray line*) are shown. *D*. Excitation signal ($e_1(t)$) for a movement in *A*. The ideal excitation signal (*black line*) and a real excitation signal (*gray line*) are shown

Figure 4. *A*. *Black lines*. Relationship between movement amplitude, duration, and variability in the presence of SDN_m ($\sigma_{SDNm} = 0.8$; $\sigma_{SDNs} = 0.0$; $\sigma_{SINm} = 0.0$; $\sigma_{SINs} = 0.02$; $\Delta = 0$). Movements of different amplitudes (A = 10-60 cm, step 2 cm) and durations (MT = 200-800 ms, step 20 ms) were simulated ($N = 500$ trials). For a given variability W ($W^2 = 1$-9 cm^2, step 1 cm^2), the relationship between A and MT was built by interpolation across amplitudes and durations. *Gray lines*. Similar results obtained with feedback delay $\Delta = 100$ ms (A = 10-60 cm, step 5 cm; MT = 200-800 ms, step 50 ms; same noise statistics; $N = 100$ trials). *Dashed lines*. Similar results obtained with $p = 1.5$ (exponent of noise). *B*. Same as *A* for SDN_m and SDN_s ($\sigma_{SDNm} = 0.5$; $\sigma_{SDNs} = 0.5$; $\sigma_{SINm} = 0.0$; $\sigma_{SINs} = 0.02$; $\Delta = 0$). *C*. Relationship between effort (arbitrary unit) and variability for data in *A* (when $\Delta = 0$). *D*. Same as *C* for data in *B*.

Figure 5. *A*. Variations in aspect ratio (*top*), surface area (in cm^2, *middle*), and orientation (*bottom*) with σ_{SDNm} for different σ_{SINs} (*circle*: 0.05; *box*: 0.1; *diamond*: 0.15). Other parameters: $\sigma_{SINm} = 0$, $\sigma_{SDNs} = 0$. *B*. Same as *A* for SDN_s. Other parameters: $\sigma_{SINm} = 0$, $\sigma_{SDNm} = 0.5$. Feedback delay was $\Delta = 0$. Movement as in Fig. 3*A*,*B*.

Figure 6. *A*. Variability for movements in 5 directions (10 cm, 400 ms) under SDN_m ($\sigma_{SDNm} = 0.5$). See Fig. 5*A* for explanations. Parameters: $\sigma_{SINm} = 0.0$, $\sigma_{SINs} = 0.1$, $\sigma_{SDNs} = 0.0$. *B*. Same as *A* for SDN_s ($\sigma_{SDNs} = 0.6$). Parameters: $\sigma_{SINm} = 0.0$, $\sigma_{SDNm} = 0.5$, $\sigma_{SINs} = 0.06$. *C*. Quantitative description of variability ellipses for data in *A*. As system dynamics is invariant by horizontal and vertical symmetry, results for 16 directions were obtained accordingly. Data were presented on a polar plot. 0 deg is on the right. From *left* to *right*: orientation, aspect ratio, surface area (normalized). The central gray circle corresponds to 0 deg (*left*), 1 (*center*), and 0.5 (*right*). *D*. Same as *C* for data in *B*. The central gray circle corresponds to 0 deg (*left*), 2

(*center*), and 0.5 (*right*). Feedback delay was $\Delta = 0$.

Figure 7. *A*. Influence of sensory delay (25-100 ms) on the characteristics of variability ellipses (*A*: aspect ratio; *B*: surface area; *C*: orientation) for the movements simulated in Fig. 5. Directions are indicated by line's width (Inset in *B*). Parameters: $\sigma_{SINm} = 0.0$, $\sigma_{SDNm} = 0.25$, $\sigma_{SINs} = 0.05$, $\sigma_{SDNs} = 0.5$.

Figure 8. Quantitative description of variability ellipses for the nonlinear model using movements in 16 directions (10 cm, 400 ms, $N = 500$ trials). Same format as in Fig. 6*C*,*D*. Initial arm posture was (40°,90°). *A*. Variability due to SDN_m ($\sigma_{SDNm} = 0.15$). Parameters: $\sigma_{SINm} = 0.0$, $\sigma_{SINs} = 0.3$, $\sigma_{SDNs} = 0.2$. Surface area was normalized. Maximum surface area was 0.44 cm^2. *B*. Variability due to SDN_s ($\sigma_{SDNs} = 0.8$). Parameters: $\sigma_{SINm} = 0.0$, $\sigma_{SDNm} = 0.15$, $\sigma_{SINs} = 0.3$. Maximum surface area was 2.2 cm^2.

Figure 9. *A*. Movement variability for $\sigma_{SDNm} = 0.7$, $\sigma_{SDNs} = 0.2$, $\sigma_{SINs} = 0.02$. 5 trajectories are shown. Inset: Enlarged view of endpoint distribution. Circle diameter is 2.5 cm. *B*. Same as *A* for $\sigma_{SDNm} = 0.8$, $\sigma_{SDNs} = 0.1$, $\sigma_{SINs} = 0.02$. Circle diameter is 1.9 cm. *C*. Time course of position variability for data in *A* (*gray*) and *B* (*black*). The plotted quantity is the square root of the surface area (in cm) of the variability ellipse at each time along the trajectory. Inset: Velocity profiles. *D*. Time course of force variability. *E*. Time course of EMG variability. *F*. Spatial variability of kinematic landmarks (pka: peak acceleration; pkv: peak velocity, pkna: peak negative acceleration). The plotted quantity is the standard deviation (in mm) of the distance to the landmark. The same movement was used in all the simulations: 45°, 30 cm, 300 ms. Statistics were made over $N = 1000$ movements. Feedback delay was $\Delta = 0$.

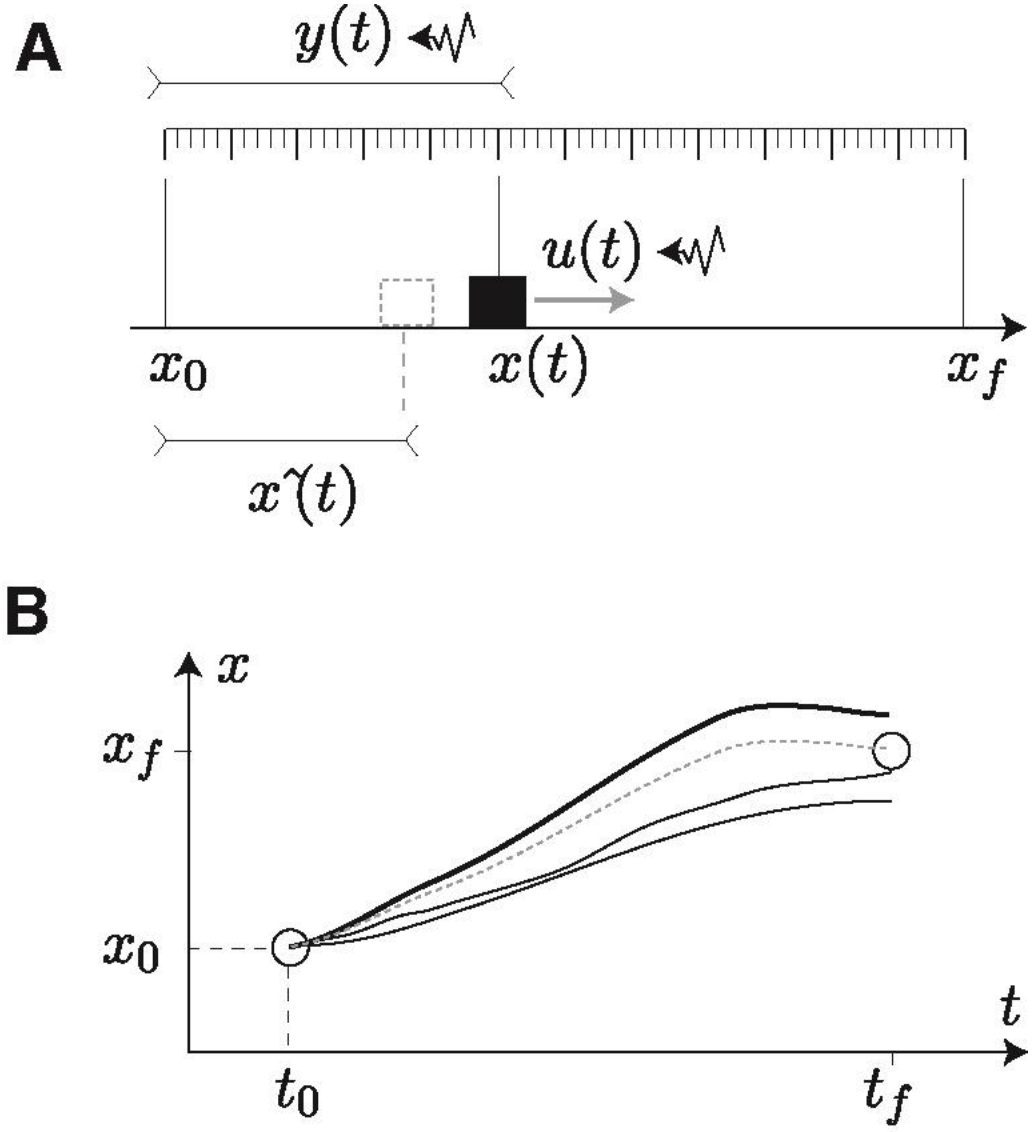

FIGURE 1

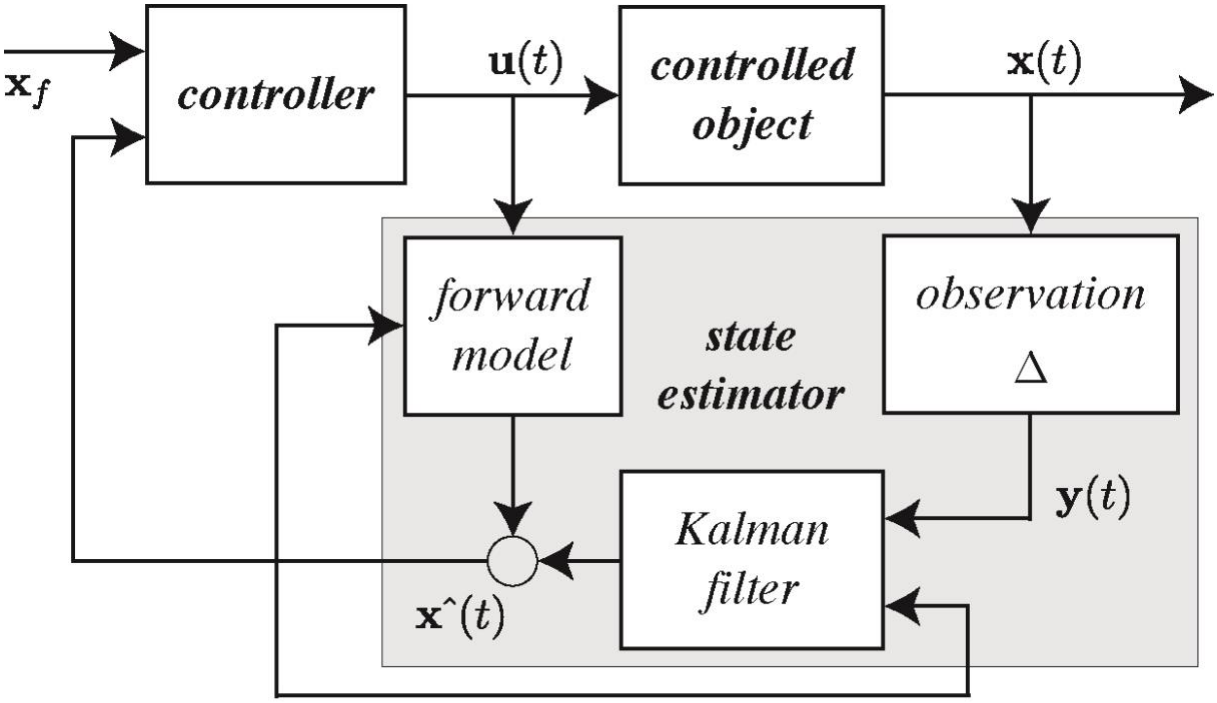
$\mathbf{x}_f$
controller
$\mathbf{u}(t)$
controlled object
$\mathbf{x}(t)$
forward model
state estimator
observation
Δ
$\mathbf{y}(t)$
Kalman filter
$\hat{\mathbf{x}}(t)$

FIGURE 2

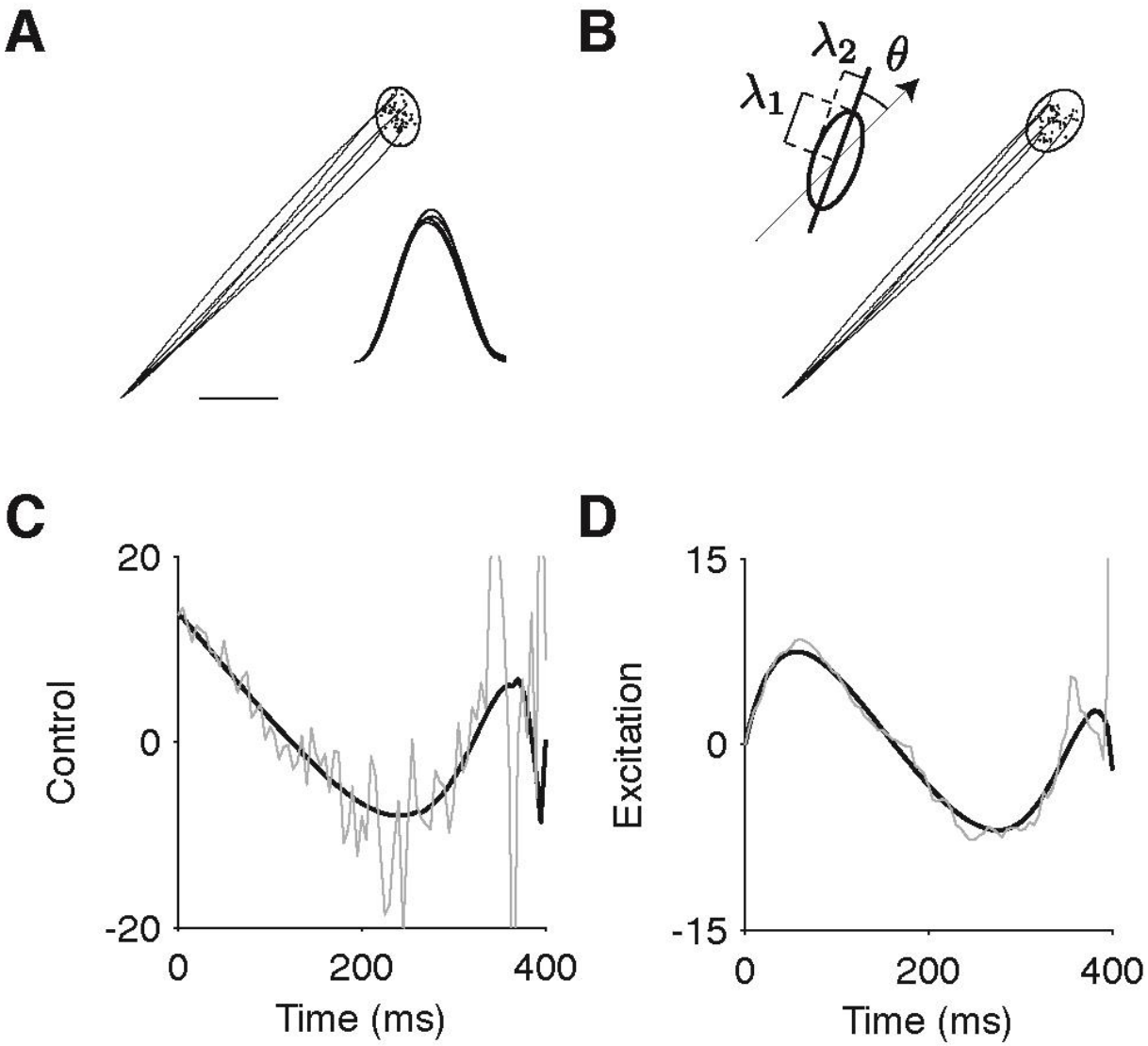
A
B
λ_2
θ
λ_1
C
D
20
0
-20
Control
0
200
400
Time (ms)
15
0
-15
Excitation
0
200
400
Time (ms)

FIGURE 3

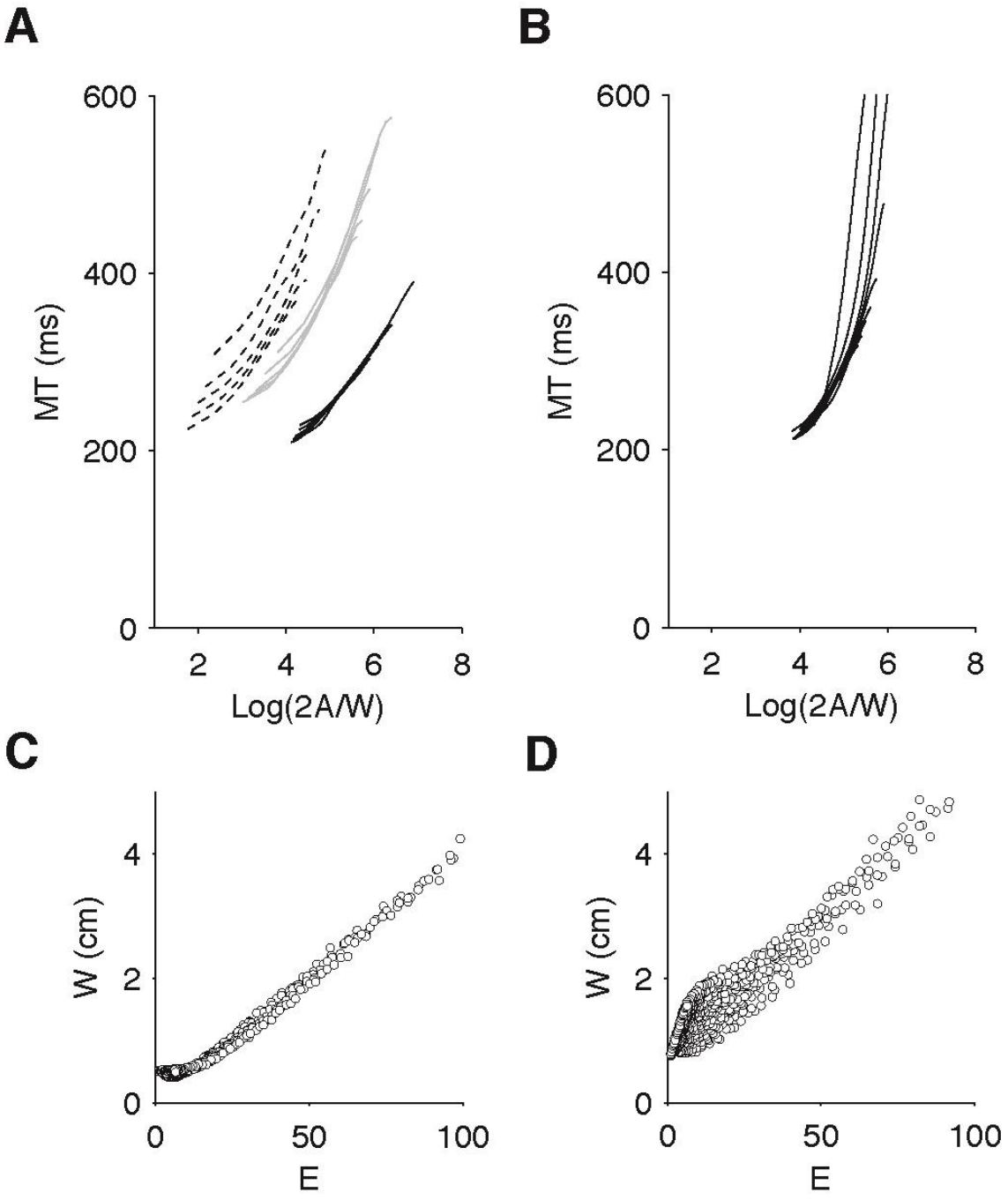

FIGURE 4

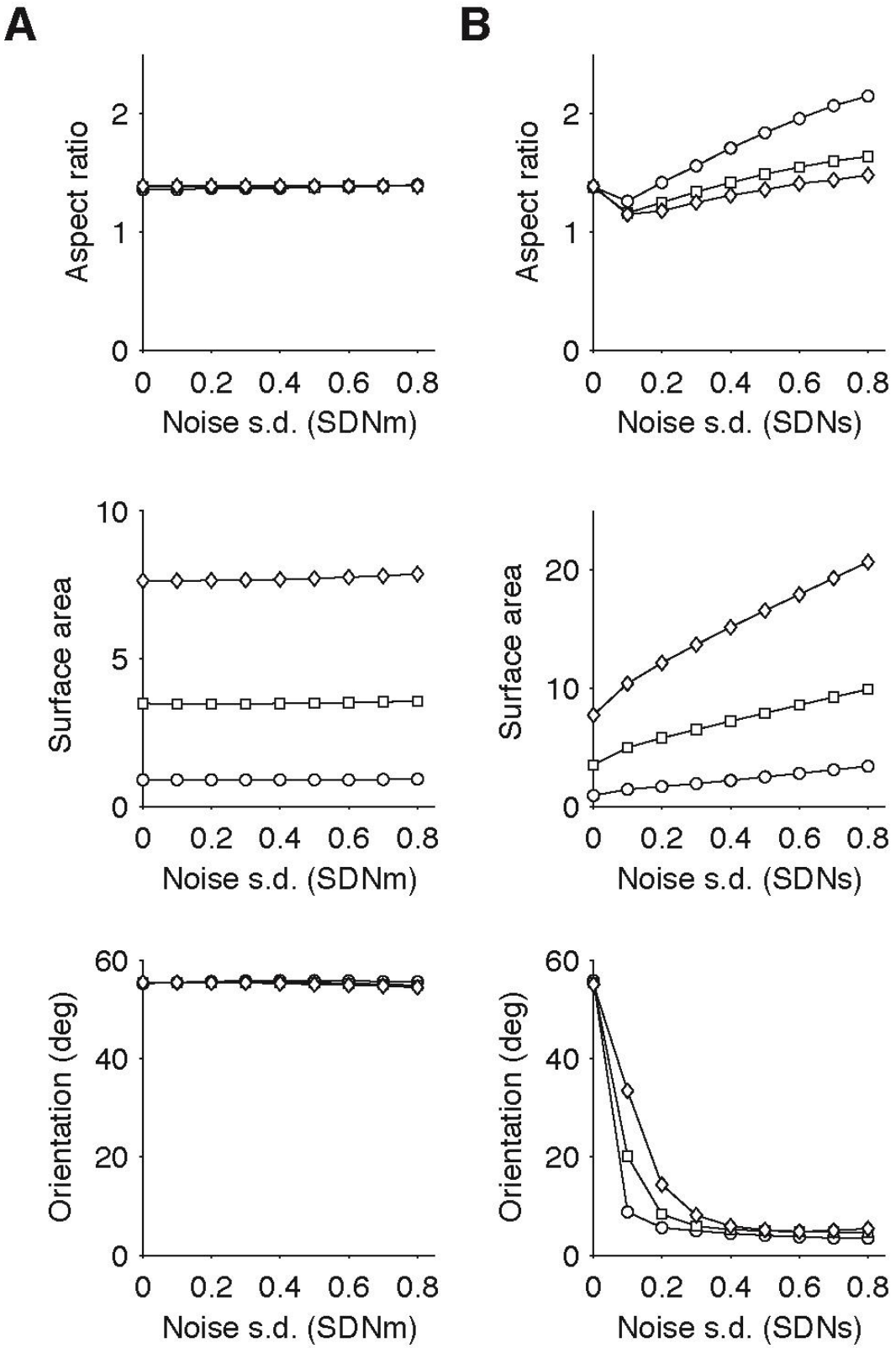
A
B
Aspect ratio
Surface area
Orientation (deg)
Noise s.d. (SDNm)
Noise s.d. (SDNs)
0
0.2
0.4
0.6
0.8
1
2
5
10
20
40
60

FIGURE 5

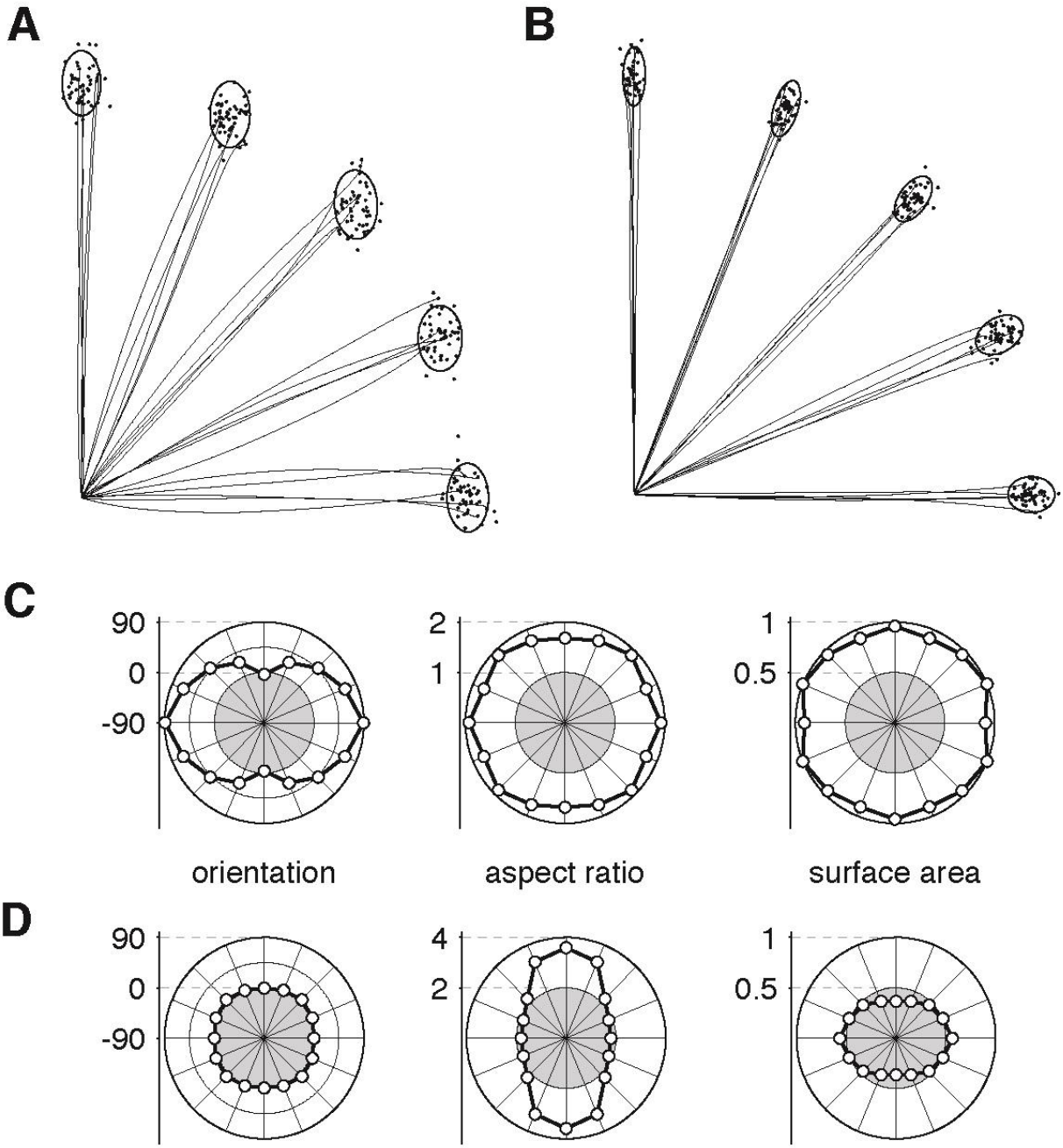
A
B
C
90
0
-90
orientation
2
1
aspect ratio
1
0.5
surface area
D
90
0
-90
4
2
1
0.5

FIGURE 6

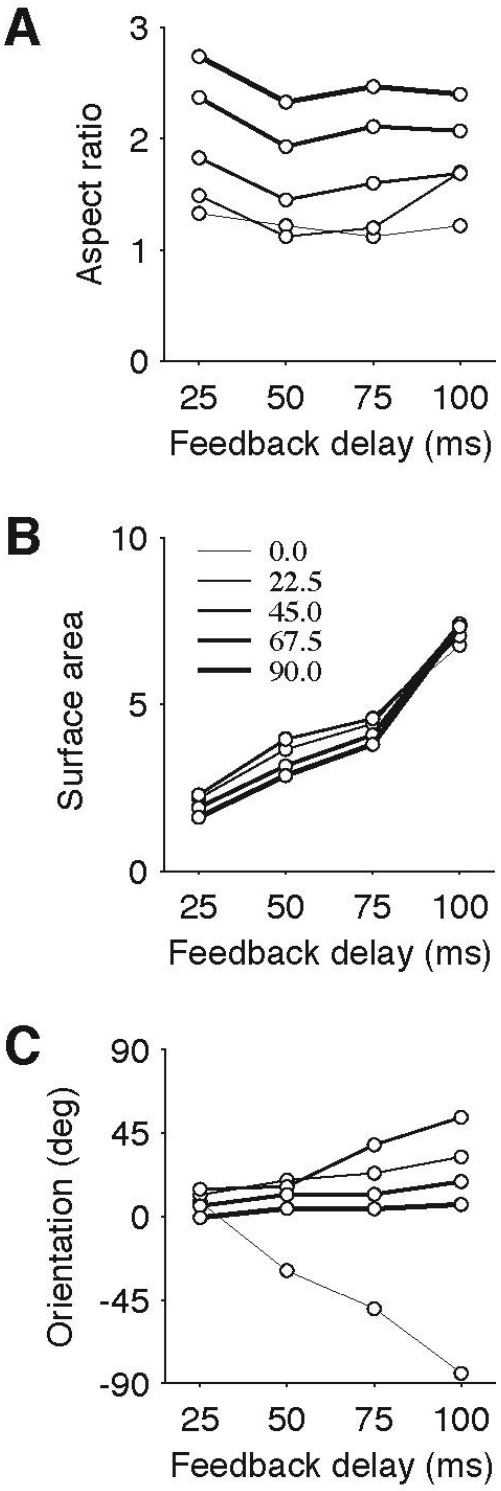
A
Aspect ratio
3
2
1
0
25
50
75
100
Feedback delay (ms)
B
Surface area
10
5
0
0.0
22.5
45.0
67.5
90.0
25
50
75
100
Feedback delay (ms)
C
Orientation (deg)
90
45
0
-45
-90
25
50
75
100
Feedback delay (ms)

FIGURE 7

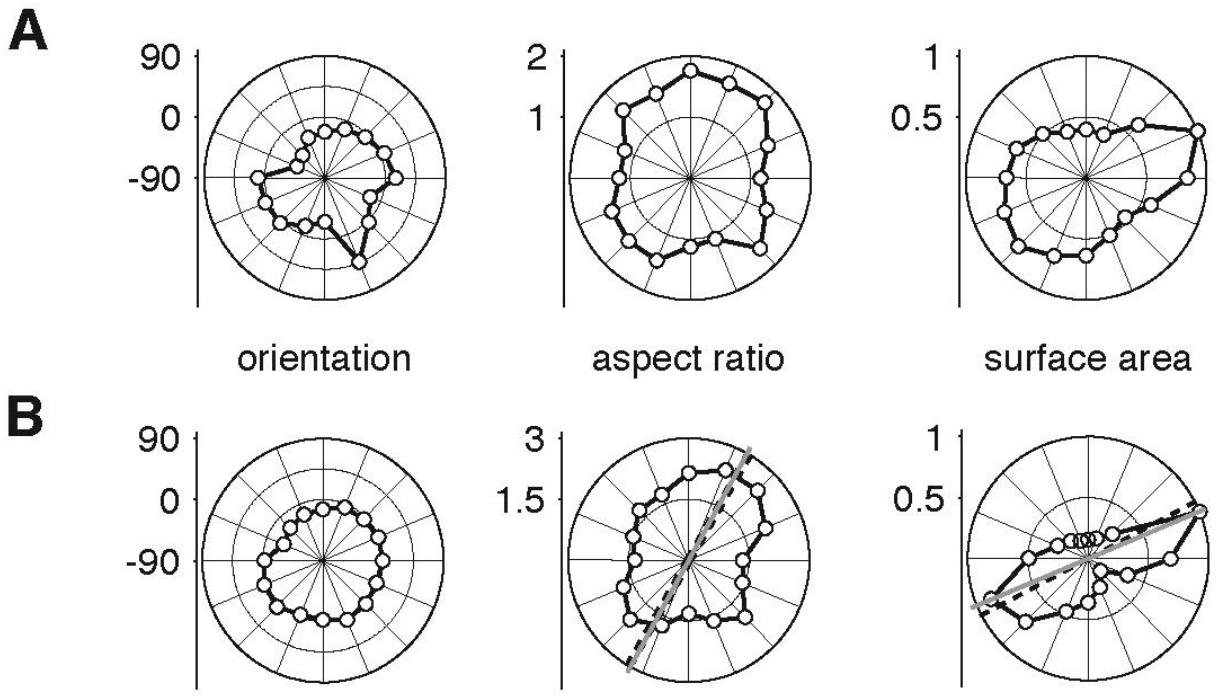
A
90
0
-90
2
1
1
0.5
orientation
aspect ratio
surface area
B
90
0
-90
3
1.5
1
0.5

FIGURE 8

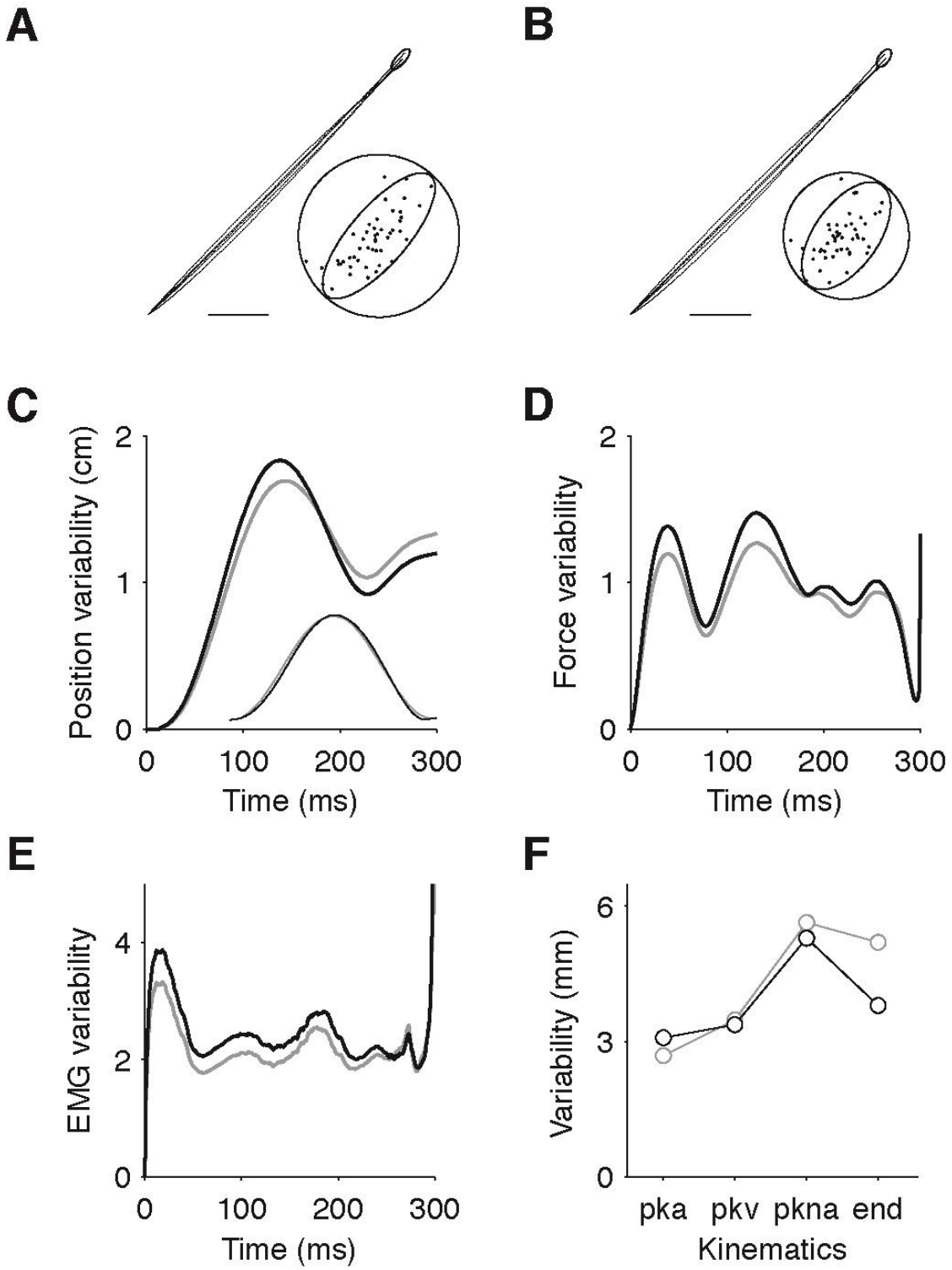
A
B
C
Position variability (cm)
2
1
0
0
100
200
300
Time (ms)
D
Force variability
2
1
0
0
100
200
300
Time (ms)
E
EMG variability
4
2
0
0
100
200
300
Time (ms)
F
Variability (mm)
6
3
0
pka
pkv
pkna
end
Kinematics

FIGURE 9